geodiversitas

2018 • 40 • 13

Early bison remains from Mygdonia Basin (Northern Greece)

Dimitris S. KOSTOPOULOS, Ioannis MANIAKAS & Evangelia TSOUKALA

art. 40 (13) — Published on 5 July 2018
www.geodiversitas.com

MUSÉUM
NATIONAL D'HISTOIRE NATURELLE
PUBLICATIONS
SCIENTIFIQUES

Couverture / *Cover* :
Réalisée à partir de la Figure 4 de cet article/*created from Figure 4 of this article.*

Geodiversitas est indexé dans / Geodiversitas *is indexed in:*
- Science Citation Index Expanded (SciSearch®)
- ISI Alerting Services®
- Current Contents® / Physical, Chemical, and Earth Sciences®
- Scopus®

Geodiversitas est distribué en version électronique par / Geodiversitas *is distributed electronically by:*
- BioOne® (http://www.bioone.org)

Les articles ainsi que les nouveautés nomenclaturales publiés dans *Geodiversitas* sont référencés par /
Articles and nomenclatural novelties published in Geodiversitas *are referenced by:*
- ZooBank® (http://zoobank.org)

Geodiversitas est une revue en flux continu publiée par les Publications scientifiques du Muséum, Paris
Geodiversitas *is a fast track journal published by the Museum Science Press, Paris*

Les Publications scientifiques du Muséum publient aussi / *The Museum Science Press also publish:*
Adansonia, ***Zoosystema***, ***Anthropozoologica***, ***European Journal of Taxonomy***, ***Naturae.***

Diffusion – Publications scientifiques Muséum national d'Histoire naturelle
CP 41 – 57 rue Cuvier F-75231 Paris cedex 05 (France)
Tél. : 33 (0)1 40 79 48 05 / Fax : 33 (0)1 40 79 38 40
diff.pub@mnhn.fr / http://sciencepress.mnhn.fr

ISSN (imprimé / *print*) : 1280-9659/ ISSN (électronique / *electronic*) : 1638-9395

Early bison remains from Mygdonia Basin (Northern Greece)

Dimitris S. KOSTOPOULOS
Ioannis MANIAKAS
Evangelia TSOUKALA
Aristotle University of Thessaloniki, Laboratory of Plaeontology, School of Geology,
54124 Thessaloniki (Greece)
dkostop@geo.auth.gr (corresponding author)
imaniaka@geo.auth.gr
lilits@geo.auth.gr

Submitted on 14 November 2017 | accepted on 12 February 2018 | published on 5 July 2018

urn:lsid:zoobank.org:pub:F370A5EE-7683-457A-BE38-93301AD6797B

Kostopoulos D. S., Maniakas I. & Tsoukala E. 2018. — Early bison remains from Mygdonia Basin (Northern Greece). *Geodiversitas* 40 (13): 283-319. https://doi.org/10.5252/geodiversitas2018v40a13. http://geodiversitas.com/40/13

ABSTRACT

The continuous enrichment of the European Pleistocene mammal fossil record leads inevitably to a comprehensive forthcoming review of the biogeographic and evolutionary history of bisons on the continent. New and revised data from the post-Olduvai (<1.8 Ma)-pre-Jaramillo (>1.0 Ma) time span of the Mygdonia basin (N. Greece), exposed here, indicate the presence of a small bison referred to as *Bison* cf. *degiulii* (Masini, Palombo & Rozzi, 2013) due to its similarities with the contemporaneous type material from the Italian Peninsula. A series of minor morphometrical changes detected across chronologically successive Mygdonia bison populations is interpreted as local adaptations to harsher environmental conditions. A re-evaluation of several morphological and biometrical features of the European early bison populations in comparison with later and extant taxa leads to the reconfirmation of some characters as taxonomically and phylogenetically important, while questioning others. The results allow recognizing *B. degiulii* as most likely member of the true bison clade *Bison* (*Bison*) Hamilton Smith, 1827 and reconsidering the current *B.* (*Eobison*) Flerov, 1972 concept. The data from Mygdonia basin and Northern Greece confirm the short co-occurrence of *Bison* Hamilton Smith, 1827 and *Leptobos* Rütimeyer, 1877-1878 in the Balkans and suggest the appearance of at least two bison lineages in Southern Europe between 1.7-1.5 Ma.

KEY WORDS
Bovini,
Bison,
Eobison,
Early Pleistocene,
palaeodemography.

RÉSUMÉ

Les restes de bison primitif du Bassin de Mygdonia (Nord de la Grèce).

L'enrichissement continuel du registre fossile mammalien du Pléistocène européen amène à la révision complète de la biogéographie et de l'histoire évolutive des bisons sur ce continent. Les données nouvelles et réexaminées de la période post-Olduvai (< 1.8 Ma)-pré-Jaramillo (> 1.0 Ma) du bassin de Mygdonia (N. Grèce) présentées dans cet article indiquent la présence d'un petit bison que l'on peut attribuer à *Bison* cf. *degiulli* (Masini, Palombo & Rozzi, 2013) de par ses similarités avec le matériel type contemporain provenant de la Péninsule italienne. Une série de changements morphométriques a été détectée au travers des populations successives des bisons de Mygdonia et interprétée comme une adaptation locale à des conditions environnementales plus rudes. Une réévaluation de plusieurs caractères morphométriques et biométriques des premières populations européennes de bisons permet de confirmer ou de remettre en question la valeur taxinomique et phylogenique de certains caractères. Les résultats permettent de reconnaître *B. degiulli* comme étant probablement un membre du clade *Bison* (*Bison*) Hamilton Smith, 1827 propre et de reconsidérer le concept actuel de *Bison* (*Eobison*) Flerov, 1972. Les données du bassin de Mygdonia et du Nord de la Grèce confirment la brève co-occurence de *Bison* Hamilton Smith, 1827 et *Leptobos* Rütimeyer, 1877-1878 dans les Balkans et suggèrent l'apparition d'au moins deux lignées de bisons en Europe du Sud entre 1,7 et 1,5 Ma.

MOTS CLÉS
Bovini,
Bison,
Eobison,
précose pléistocène,
paléodémographie.

INTRODUCTION

Bison Hamilton Smith, 1827 has been for a long time marked as one of the most iconic animal figures of the Eurasian and Nord American mid-Pleistocene to historical times. Until the late 80's, the European bison record ran back as far as the beginning of the Middle Pleistocene, suggesting a late invasion and a rather simple evolutionary history (e.g. Sala 1987 and references therein). Over the next years, the discovery of an important number of new Lower Pleistocene European fossil localities revealed a wealth Early Pleistocene bison record (e.g. Moyà-Solà 1987; Masini 1989; Brugal 1995; Kostopoulos 1997; Sher 1997), postdating significantly the genus expansion into the (sub-)continent. Deeply influenced by the earlier works of Flerov (1972, 1979), most scholars directly or indirectly ascribed these early European bison population to *Bison* (*Eobison*) Flerov, 1972, a subgenus of Asian origin but of unknown phylogenetic and disputable taxonomic concepts. The spatial and time discontinuity of the Early Pleistocene European fossil record triggered diverging new hypotheses on the intrageneric relationships and systematics of European *Bison* (e.g. Sher 1997; Bukshianidze 2005; Croitor 2016; Made *et al.* 2017), further exaggerated by the conflicting molecular data and neontological opinions (e.g. Verkaar *et al.* 2004; Groves & Grubb 2011; Hassanin *et al.* 2013; Massilani *et al.* 2016; Soubrier *et al.* 2016). The timing and ecological background of bison invasion in Europe came also at the center of several discussions as they presumably coincide with the replacement of typically Villafranchian large bovines, such as *Leptobos* Rütimeyer, 1877-1878 and the arrival of *Homo* Linnaeus, 1758 (e.g. Made *et al.* 2017).

Till the 90's evidence of Greek fossil bison was scarce, based mainly on a few remains from the Mid-Late Pleistocene faunas of Megalopolis Basin in Peloponnesus and Petralona cave in northern Greece (Melentis 1966; Tsoukala 1989). Later on, an important bison sample was recovered from the Lower Pleistocene locality of Apollonia in Mygdonia Basin, N. Greece (Kostopoulos 1997). The material referred to as *Bison* (*Eobison*) sp. due to its primitiveness but the lack of crania and the poorness of the European record prevent at that time a precise species identification. Extensive fieldwork in Mygdonia Basin during the last two decades unearthed important bison material from new localities such as Kalamoto and Tsiotra Vryssi (Tsoukala & Chatzopoulou 2005; Konidaris *et al.* 2015) and further improved the bison record from the Apollonia fossil site. New data described here and revised old ones, permit: 1) re-evaluating the taxonomic identity of the Greek early bisons in comparison with the Eurasian bison record; and 2) re-assembling their biochrological trail. The concept of *Eobison* and its European record are discussed. An appendicular palaeodemographic analysis of the best documented Apollonia bison population is also provided.

MATERIAL AND METHODS

The studied bison material comes from four fossiliferous sites, located in the Mygdonia Basin of Northern Greece (Fig. 1), namely Kalamoto-2 (KLT), Krimni (KRI and KRM), Tsiotra Vryssi (TSR) and Apollonia-1 (APL) (Koufos *et al.* 1995; Kostopoulos 1997; Tsoukala & Chatzopoulou 2005; Konidaris *et al.* 2015). TSR, KRM/KRI, and KLT are placed in the uppermost stratigraphic levels of the red-beds of the Gerakarou Formation (Fm), whereas APL is placed in the lowermost sandy parts of the succeeding Platanochori Fm of mostly grey-green silts. All the material, apart from that of KLT, is stored in the Museum of Geology and Paleontology of the Aristotle University of Thessaloniki (LGPUT). KLT material is housed in the Natural History Collection of Kalamoto, Kalindoia, Lagada, Greece (NHCK).

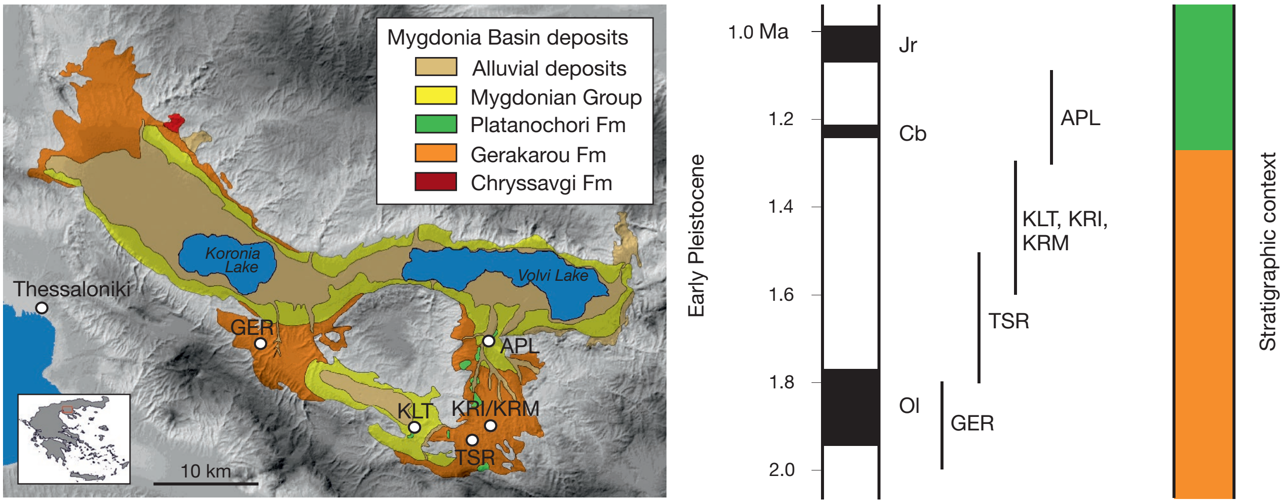

FIG. 1. — Geographic, geological, and chronological context of the fossiliferous sites from Mygdonia Basin yielding early *Bison* Hamilton Smith, 1827 and *Leptobos* Rütimeyer, 1877-1878 remains. Abbreviations: **Fm**, Lithostratigraphic Formation; **APL**, Apollonia-1; **TSR**, Tsiotra Vryssi; **KRI/KRM**, Krimni; **KLT**, Kalamoto-2; **GER**, Gerakarou; **Ol**, Olduvai (geomagnetic field) reversal; **Cb**, Cobb mountain reversal; **Jr**, Jaramillo reversal. Map courtesy of D. Giusti (Eberhard Karls University of Tübingen, Senckenberg Center for Human Evolution and Palaeoenvironment).

The taxonomic history of extant Bovina is quite complicated and highly confusing, largely reflecting the problems arising from a rapid radiation between 4 and 2 Ma and possibly repeated introgression phenomena (Geraads 1992; Verkaar *et al.* 2004; MacEarchern *et al.* 2009; Groves & Grubb 2011; Zeyland *et al.* 2012; Hassanin *et al.* 2013; Soubrier *et al.* 2016). Based on morphological and molecular data of Holocene and extant Bovini, Groves & Grubb (2011), Hassanin (2014) and others propose the inclusion of all extant Bovina in a single genus *Bos* Linaeus, 1758. Abandoning, however, the generic name *Bison* is not an easy task as it has a long tradition in neontological and paleontological studies and it appears well-established in the popular sense (see also discussion in Plumb *et al.* 2014). Additionally, the adoption of *Bos* (*Bison*) leaves taxonomically orphan a series of fossil samples of primitive bisons, representing a rank greater than the species but less than the genus. Instead, we adopt here a classification scheme extrapolating the results of a recent phylogenetic analysis conducted by Hassanin *et al.* (2013) based on multiple autosomal introns (see also Xie *et al.* 2010). Within this scheme, three Bovina lineages of genus value would be recognized: *Bos* (including fossil and living representatives related to aurochs and banteng), *Bison* (including wisent, bison, yak and their fossil allies), and *Bibos* (Hodgson, 1837) (including only the gaur or Indian bison and its domesticated variant, as originally proposed by Hodgson 1837). The closely related and recently split (*c.* 230 ka, according to Scott 2010) American bison and the European wisent are placed within the subgenus *Bison* (*Bison*), which in its turn and congruently with morphological data (e.g. Groves 1981; Geraads 1992) is recognized as the sister group of *Bison* (*Poephagus*) (Gray, 1843), including fossil and living yaks (i.e., *Bison* (*Poephagus*) *baicalensis* Veretchgagin, 1954; *Bison* (*Poephagus*) *mutus* Przewalski, 1883). *Bison* (*Eobison*) is considered as a third stem lineage of the same clade.

The present study focus on cranial, dental and metapodial material. Linear measurements were taken with a digital caliper at 0.01 mm precision. Angles were measured with a digital goniometer of 0.1° precision. Upper case letters (P, M) are for upper toothrows and teeth and lower case letters (p, m) for lower ones; a D/d before them marks a deciduous upper/lower tooth.

Descriptions of cranial and dental features follow standard terminology with minor additions (e.g. Masini 1989; Bukshianidze 2005; Bärmann & Rössner 2011; Cherin *et al.* 2017). Measurements of crania and horncores follow Masini (1989) (see also Cherin *et al.* 2017). Tooth and toothrow lengths (L) are measured on the occlusal surface, whereas tooth breadths (W) close to the basal-most exposed part of the crown, both values representing teeth's maximum preserved dimensions. As a result wear stages are indirectly reflected on the measured molar lengths only, which gradually reduce with age. Measured heights (H) represent the buccal maximum height of the paracone for the upper molars and the lingual maximum height of the metaconid for the lower molars. Relative hypsodonty is estimated here as the height of the crown at the paracone (for the upper unworn molars) or metaconid (for the lower unworn molars) divided by the occlusal (available maximum) length of the tooth. Metapodial measurements and measurement abbreviations are according to Scott (2004; see Maniakas & Kostopoulos 2017a: fig. 2).

An extant bison equivalent age (EBEA) for each fossil individual represented by craniodental remains is estimated by reference to the eruption and wear dental stages of *Bison bonasus* (Linnaeus, 1758) provided by Wegrzyn & Serwatka (1984) and *Bison bison* (Linnaeus, 1758) provided by Skinner & Kaisen (1946), calibrated through a set of ten *B. bonasus* crania of different sexes and ontogenetic stages stored in the Senckenberg Center for Human Evolution and Paleoenvironment, Archaeozoology collection, University of Tübingen (HEP-AcUT).

TABLE 1. — Sex identification of the cranium KLT-638 according to ten selected criteria (see Appendix 1). Symbol: *, although the dorsal part is totally missing the preserved lateral part of the maxillary bones indicate a voluminous maxilla; the index "maximum width of the cranium at the maxilla against biorbital width" is 1.45, certainly smaller than both adult males and females of *B. bonasus* (Linnaeus, 1758) but high comparatively to other contemporaneous bison crania.

	1	2	3	4	5	6	7	8	9	10
KLT-638	? ♀	♀	♀	*c.* ♂	♀	*c.* ♀	*c.* ♀	?♀*	?	*c.* ♀

Body mass estimations are provided from a set of equations available in the literature and based either on the M1 area or on metacarpal metrical variables (for methodology and references see Maniakas & Kostopoulos 2017a). In the latter case we preferred a mixed herd (males and females) average body mass estimation (ABME) resulting from the three individual body mass estimations produced by PML (mediolateral diameter of the proximal epiphysis), PAP (anteroposterior diameter of the proximal epiphysis), and IDML (greatest mediolateral diameter of the inferior aspect of distal epiphysis) linear variables of metacarpals (following Scott 1983; for linear measurements on metapodials see Maniakas & Kostopoulos 2017a: fig. 2).

Sex identification of early bison crania is quite difficult as common criteria extracted from Late Pleistocene and extant bison taxa are not fully applicable here. Early bison crania lack typical adult features exaggerated in males of later and living taxa such as the tubular eye sockets, the massive and long horncores, the pneumatized frontals etc. (Gromova 1935; Schertz 1936; Skinner & Kaisen 1946; Empel 1962; Flerov 1979; Sala 1987; Vasiliev 2008; Kobryńczuk *et al.* 2008), while other sexual features such as the early closing of cranial sutures in males are hardly detectable on fossils. Sala (1987) and Sher (1997) already discussed possible heterochrony phenomena in bisons, and it is accepted here that adult crania of early taxa appear, as a rule, more juvenile-like (and also feminine-like) compared to Late Pleistocene, Holocene and modern ones. In order, therefore, to determine the sex of early bison crania, we use here a combination of ten characters provided either in the literature (Skinner & Kaisen 1946; Empel 1962; McDonald 1981) or from original observations on a set of ten European wisent crania of both sexes (stored at HEP-AcUT; Appendix 1).

Metapodial bivariate and multivariate metrical analyses are based on data and methodology already introduced in Maniakas & Kostopoulos (2017a) with small additions and modifications. In order to eliminate the size effect on PCA analyses, a Mosimann's Log-Shape ratio transformation of data has been performed (i.e., by dividing each value with the specimen's geometric mean and logarithmizing the results). Statistical elaboration of data was performed with PAST (Hammer *et al.* 2001).

Appendix 2 presents most taxa in question known by cranial elements. Other European samples, documented mostly by dental and/or postcranial elements take also part of the forthcoming discussion.

ABBREVIATIONS

Institutions

HEP-AcUT	Senckenberg Center for Human Evolution and Palaeoenvironment, Archaeozoology collection, University of Tübingen;
LGPUT	Laboratory and Museum of Geology and Paleontology, Aristotle University of Thessaloniki;
NHCK	Natural History Collection of Kalamoto, Kalindoia, Langada, Greece.

Localities

APL	Apollonia 1;
KLT	Kalamoto 2;
KRI/KRM	Krimni;
TSR	Tsiotra Vryssi.

Technical

ABME	mixed herd average body mass estimation;
EBEA	extant bison equivalent age;
L	tooth and toothrow length;
H	height;
W	breadth;
DAP	rostrocaudal (anteroposterior) diameter of horncore base;
DVD	dorsoventral diameter of horncore base.

Additional metrical abbreviations are given in Table 2 (for cranium) and Appendix 3 (for metapodials).

SYSTEMATIC PALAEONTOLOGY

Order MAMMALIA
Family BOVIDAE Gray, 1821
Subfamily BOVINAE Gray, 1821
Genus *Bison* Hamilton Smith, 1827

Subgenus *Bison* Hamilton Smith, 1827

TYPE SPECIES. — *Bos bison* Linnaeus, 1758 by subsequent designation (Hamilton Smith 1827).

Bison (*Bison*) cf. *degiulii* (Masini, Palombo & Rozzi, 2013)
(Figs 2-7)

REMARKS

The binomial *Eobison degiulii* was originally introduced by Masini (1989: 54) in a dissertation thesis by the University of Modena and Florence (Italy), which, according to the International Code of Zoological Nomenclature (ICZN 1999: arts 8, 9), does not meet the criteria of formal publication. The species appears in its original combination or as *Bison* (*Eobison*) *degiulii* or as *Bison degiulii* in several following works by multiple authors without, however, being associated by any formal nomenclature act. It re-appears in the periodical journal *Quaternary International* by Masini *et al.* (2013: 53) as '*Bison* (*Eobison*) *degiulii* Masini (1989)' associated by a holotype designation (Masini *et al.* 2013: fig. 9), illustrations, a description of basic cranial features and comparisons, altogether constituting sufficient elements of an available

Table 2. — Cranial measurements of KLT-638 in comparison with other related taxa (data from Masini 1989; Bukshianidze 2005).

			Bison			
Cranial Measurements	**Abbr.**	**KLT-638**	***B. degiulii*** **(Masini, Palombo & Rozzi, 2013)**	***B. georgicus*** **(Burchak-Abramovich & Vekua, 1994)**	***B. palaeosinensis*** **Teilhard de Chardin & Piveteau, 1930**	***Leptobos etruscus*** **(Falconer, 1859)**
Length Nasion-Bregma	LNB	175.0	194.0	147.5	–	202.0
Chord: posterior margin of orbits to the anterior margin of horncores	LpOaHC	60.0	65.0	–	–	110.5
Distance between horncores (caudal)	DTHC	188.0	153.0	195.0	275.0	350.0
Cranial Width at the posterior margins of orbits	Ect-Ect	240.0	277.0	244.0	–	284.0
Width of Frontals at the postorbital constrictions	WFpO	202.0	239.5	241.8	237.0	267.4
Minimum Distance between the temporal fossae	Wtem	111.0	126.7	(100)	–	126.5
Distance between the supraorbital foramina	DTSupO	122.0	134.3	127.4	161.0	125.0
Anteroposterior diameter of orbit	DAPO	73.0	–	77.6	–	69.5
Height of orbit	HO	56.5	–	–	–	62.0
Length Bregma-Opisthion	LBOp	47.5	83.0	74.0	60.5	91.4
Cranial Width at mastoids	Wmas	165.0	204.0	231.0	224.0	209.4
Basal Anteroprosterior diameter of horncores	DAPHC	58.0	72.0	92.1	85.0	184.5
Basal Dorsoventral diameter of horncores	DVDHC	50.0	59.0	73.6	78.2	71.5

nomenclature act in a published work under ICZN (see also Croitor 2016).

The Kalamoto (KLT) sample

STUDIED MATERIAL . — Partial cranium, KLT-638; right upper toothrow with P2-M3; left upper molar, KLT-869; left P4(emerging)-M3, KLT-319; left lower toothrow with p2-m3, KLT-318; left lower toothrow with p3-m3, KLT-177; right metacarpal III+IV, KLT-305, 646; right metatarsal III+IV, KLT-345.

DESCRIPTION

Part of cranium, KLT-638

Part of the basioccipital, the occipital, the complete mastoids and tympanic bullae, and the anterior part of the muzzle are missing (Fig. 2). Horncores are also not preserved apart from their very basal part, which is severely damaged. The cranium does not show any plastic deformation but the surface is extensively cracked, so tracing suture lines is in most cases impossible. The specimen belongs to a mature individual: permanent upper premolars are fully established, P4 and M3 are at a moderate wear stage, the M1 entostyle starts to vanish and the M3 entostyle remains as a loop (Fig. 2F); it corresponds to a more than 60 months individual in European bison equivalent age (Wegrzyn & Serwatka 1984) and at the beginning of stage S3 (full maturity) of American bison (Skinner & Kaisen 1946), likely having an EBEA between 6 and 10 years. Though not detectable throughout their lengths, the sagittal suture is still open and the coronal suture seems partially obliterated (Fig. 2B). Interparietal-parietal suture is completely obliterated and raised as a blunt crest.

According to our sexual character analysis (Table 1), KLT-638 represents most likely a female individual. Based on the M1 area (according to Legendre's 1986 predictions), a body mass at about 515 kg is estimated for KLT-638, placing this individual within the lower (female) spectrum of body mass range estimated for the Apollonia bison (see below). Cranial measurements are given in Table 2.

The central part of the dorsal surface above the orbits (and most likely around the frontonasal region) is significantly vaulted (in transverse sense Fig. 2B: profile [1]); the cranial roof becomes then flat to slightly concave till the back of the horncores and slightly convex at the parietal region (Fig. 2B: profiles [2]-[5]). Hence, frontals appear not pneumatized between the horncores and there is no frontal ridge connecting the horncore bases. The supraorbital foramina are placed behind the orbits, spaced widely apart and sunken in rather deep (*c.* 11 mm) and narrow (6-9 mm) grooves that are largely widening and shallowing rostrally before disappearing at the level of the anterior margins of the orbits (in Fig. 2B the undistorted left one). The flexion between frontal and parietal region is weak (*c.* 146°) and that between parietal and occipital slightly obtuse (*c.* 110°) (Fig. 2B-D, profiles [4]-[5]). In occipital view, the cranial roof is not raised above the nuchal crest (Fig. 2E).

The horncores are inserted caudo-laterally and rather close to the orbits, hence the profile of the postorbital constriction is strongly convex (Fig. 2B-E). The pedicles are short, weakly pneumatized (slightly inflated dorsal profile) and together with the preserved basal part of the horncores direct laterally-posterolaterally and bend immediately downwards without rising above the frontal level. Each horncore diverges at an angle of 60° from the sagittal plane. The horncores are rather small compared to the cranium size (Table 2) and weakly compressed dorsoventrally (the index DVD/DAP is 83-89). They possibly curve quickly upwards and taper fast.

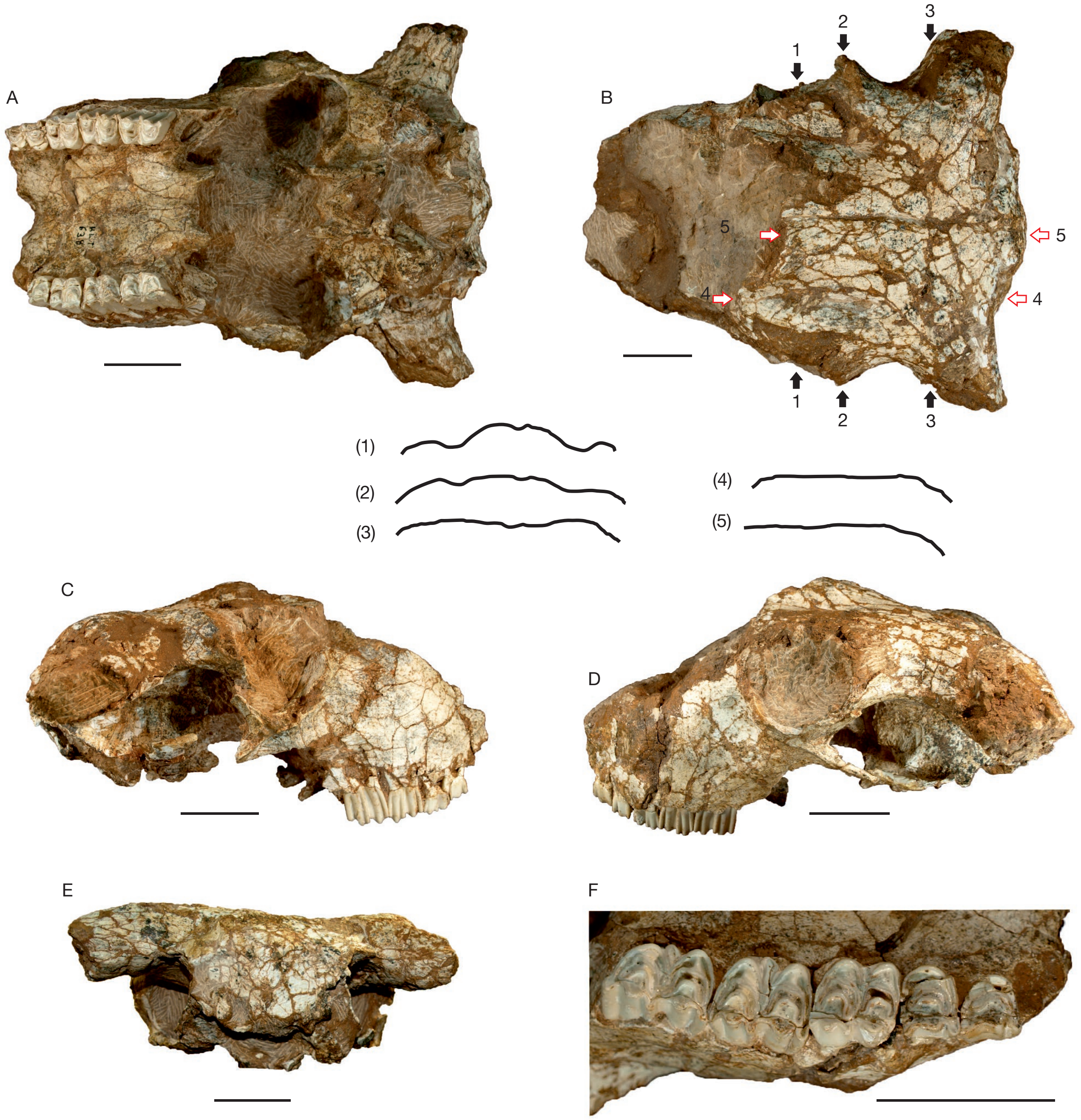

Fig. 2. — Cranium KLT-638 of *Bison* cf. *degiulii* (Masini, Palombo & Rozzi, 2013), from Kalamoto, Greece in ventral (**A**), dorsal (**B**), right lateral (**C**), left lateral (**D**) and occipital (**E**) views; **F**, close up of the left upper tooth row in occlusal view. Lines (1-5) represent dorsal transverse (1-3) and sagittal (4-5) profiles in positions indicated by arrows in (**B**). Scale bar: 5 cm.

The greater rostrocaudal axis of the horncore base is trending parallel to the frontals. The lowermost preserved point of the ventral surface of the horncores is at the level of the lower edge of the external occipital protuberance.

The bregma is clearly traceable and the coronal suture forms an angle of about 100°. Although rostrocaudally short, the parietals are clearly visible in dorsal view (Fig. 2B), taking part of the formation of the cranial roof; they continue almost flat laterally. The intertemporal bridge is very narrow (greatest width at the central part and along the sagittal plane is estimated at 35 mm) (Fig. 2B, E). The temporal crests are short, moderately developed, and not thickened (*c.* 6 mm). The temporal fossae (Fig. 2C, E) are narrow and deep and turn slightly upwards at their caudal part. The minimum distance between the hint ends of the temporal fossae is less than half of the maximum cranium width at the back of the orbits (110.0 vs 240.0 mm, respectively; Table 2). The nuchal crest is weak and its upper part is placed lower than the frontal surface (Fig. 2E). The occipital surface has a roughly trapezoidal outline and is moderately undulated (Fig. 2E); the external occipital protuberance is well developed and wide (height: 31.0 mm; width: 42.0 mm), accompanied on

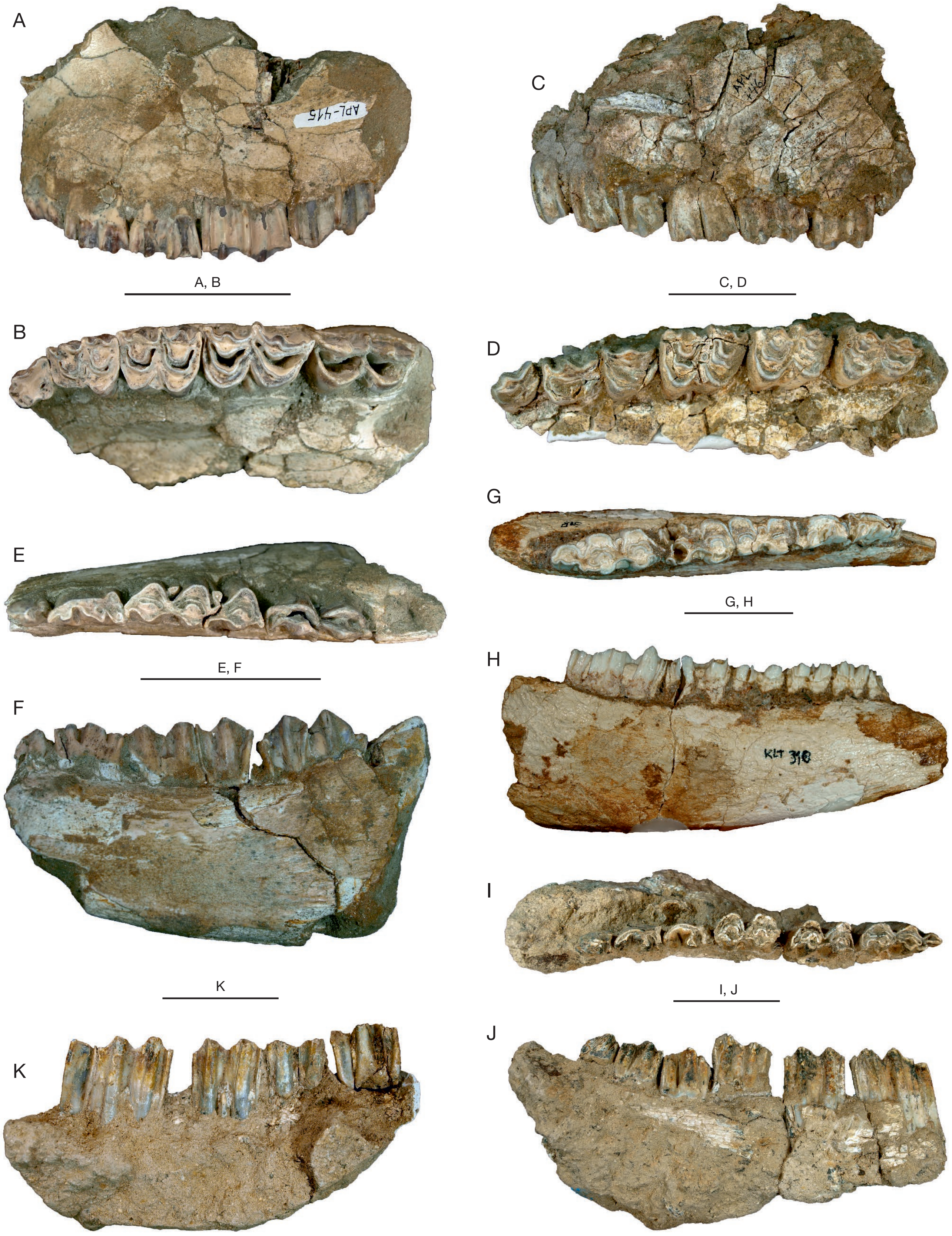

FIG. 3. — Dental remains of *Bison* cf. *degiulii* (Masini, Palombo & Rozzi, 2013) from Mygdonia Basin, Greece: **A**, **B**, left upper toothrow with dP2-M2, APL-415, buccal (**A**) and occlusal (**B**) views; **C**, **D**, left upper toothrow with P2-M3, APL-446, buccal (**C**) and occlusal (**D**) views; **E**, **F**, right mandible with dp3-m1, APL-420, occlusal (**E**) and lingual (**F**) views; **G**, **H**, left mandible with p3-m3, KLT-318, occlusal (**G**) and lingual (**H**) views; **I**, **J**, right mandible with p2-m3, TSR F20-16, occlusal (**I**) and lingual (**J**) views; **K**, left mandible with p4-m3, TSR D20-8, lingual view. Scale bar: 5 cm.

Table 3. — Hypsodonty index (height against occlusal length) in Mygdonia early bison.

Hypsodonty Index	TSR	KLT	APL
M1	–	–	1.27 (APL-497) 1.50 (APL-458) 1.55 (APL-191)
M2	–	1.44 (KLT-319)	1.58 (APL-495)
M3	–	1.60 (KLT-319)	1.63 (APL-417) 1.63 (APL-240)
m1	1.77 (TSR E18-13)	–	1.50 (APL-754) 1.75 (APL-753)
m2	–	–	1.78 (APL-456)

both sides by wide and moderately deep ligament depressions (Fig. 2E). Though strongly damaged, the mastoid appears to have a strongly convex lateral outline with thick lower part, well covering the base of the jugular process (Fig. 2E).

The basioccipital is not preserved apart of its rostral part (Fig. 2A). The anterior tuberosities of the basioccipital are rather strong (estimated length: 31.0 mm; width: 17.0 mm) and converge rostrally. The foramen oval opens just below of them, is facing laterally and it is oval shaped and moderately large (length: 11.5 mm; height: 8.4 mm). The body of the basisphenoid is strongly bent upwards compared to the basioccipital (110°). The muscular processes of the temporal bones are strong and direct mostly ventrally and weakly rostrally. The glenoid fossa is elliptic shaped, 37.8 mm wide and almost flat (Fig. 2A); its posterior margin is situated immediately below the anterior edge of the horncore base.

The orbits are large, rather rounded and not tubular but weakly protruding laterally at their caudal parts (Fig. 2B, D); their anteriormost end is placed above the posterior lobe of the M3. A shallow and rather round depression appears on jugal, just in front of the rostrodorsal part of the orbital margin (Fig. 2C, D). A sharp crest is running under the orbit and the zygomatic arches gently converge each other caudally. The facial crest is sigmoidal and especially well-marked above P2-P3, where appears parallel to the alveolar level, and above M1, where it has an almost vertical orientation.

The palate is wide, weakly concave transversally and broadens slightly in caudo-rostral direction (width at the back lobe of M3: 83.0 mm; width at P3: 88.0 mm; Fig. 2A). The palatine foramina are placed directly on the transverse palatine suture and at the level of the back lobe of M2 (Fig. 2A). The staphylion is "open-U" shaped with flattened rostral border and it is placed 12 mm behind M3 and more caudally compared to the lateral palatine indentations (Fig. 2A). The vomer is not fused with the palate.

Dentition

Apart from the cranium KLT-638 (Fig. 2F), two more upper toothrows are preserved, both belonging to relatively young individuals (measurements are given in Appendix 3A). In KLT-869 the M3 is just rising, and the P3 and P4 still within the alveolus, suggesting an EBEA of 3.5 years. The M1-M3 length is 87.0 mm. The infraorbital foramen opens above the P2 and it is large and pocketing. In KLT-319 the M3 is not worn and the P4 just erupted, suggesting an EBEA of approximately 4 years; the M1-M3 length is 93.7 mm. The length of the upper molar row is 78.4 mm on the left and 78.6 mm on the right side of the specimen KLT-638. A significant reduction of molar length with age is revealed. The upper molars are fairly hypsodont (hypsodonty index: ≥1.4 for M2 and 1.6 for M3 of KLT-319; Table 3) and typically bovine in appearance with strong and high entostyles, especially on M2 and M3 where they reach 83% and 71% respectively of the total crown height (based on the specimen KLT-319). The entostyles are attached mainly on the anterior flange of the hypocone. The molars are weakly to moderately covered by cement (accidentally removed from KLT-638), and the labial pillars and styles are strong, with the parastyle stronger than the meso- and metastyle. The distal face of M3 bears a distinct vertical groove marking the strongly projecting distolabially metastyle (Fig. 2F). The mesial lobe of the upper molars is shorter and more lingually shifted compared to the distal one. An enamel fold is present both on the distal wall of the anterior and posterior fossette of the less worn teeth. An enamel islet is also present on the M2 of KLT-869 and on the M2 and M3 of KLT-638 (Fig. 2F). The lingual cusps are well rounded. The upper premolars are rather simple with a strong parastyle. The P4 is more symmetrical (semi-elliptical in occlusal view) than the P3 and P2. The paracone pillar is strongly acute on P2, less on P3 and much less on P4. In the unworn P2 and P3 of KLT-869 the central fossette is distally divided by a moderately developed spur.

Both preserved mandibular ramii KLT-318 (Fig. 3G, H) and KLT-177 belong to old individuals, with an EBEA between 8 and 10 years (measurements given in Appendix 3B). KLT-318 mandible is about 7% deeper (at the level of p4-m1 contact) and its teeth about 15% larger than those of KLT-177. Additionally, on KLT-177 the p2 seems to be missing naturally, possibly suggesting an abnormal individual. The lower molars are characterized by thick cement cover, strong and wide lingual pillars (metaconid and entoconid) separated by a wide, "open-U" shaped valley (Fig. 3G). The parastylid is strongly projecting (at least on m3), the protoconid and hypoconid are wide, both laterally constricted and labially flattened and the ectostylid is moderately developed and attached mainly on the posterior flange of the protoconid. An additional labial stylid between the second and the third lobe is present on the m3 (Fig. 3G). The hypoconulid is distolingually marked by a rather strong stylid (more pronounced in KLT-318). A distinct distal spur is present on the posterior fossette of m3 and an entostylid on the upper part of the crown of the same tooth. On both preserved p4, the thin parastylid is weakly distinguished from the more perpendicular to the mesiodistal axis paraconid. The hypoconid is very narrow, directs distolabially and is separated from the protoconid by a narrow groove. The entoconid and the entostylid are fused (at this advanced stage of wear) in a single narrow and distolingually directed cuspid. The metaconid is strong, directed or curved strongly distolingually and with a flattened lingual wall. The anterior valley, though open and V-shaped, closes

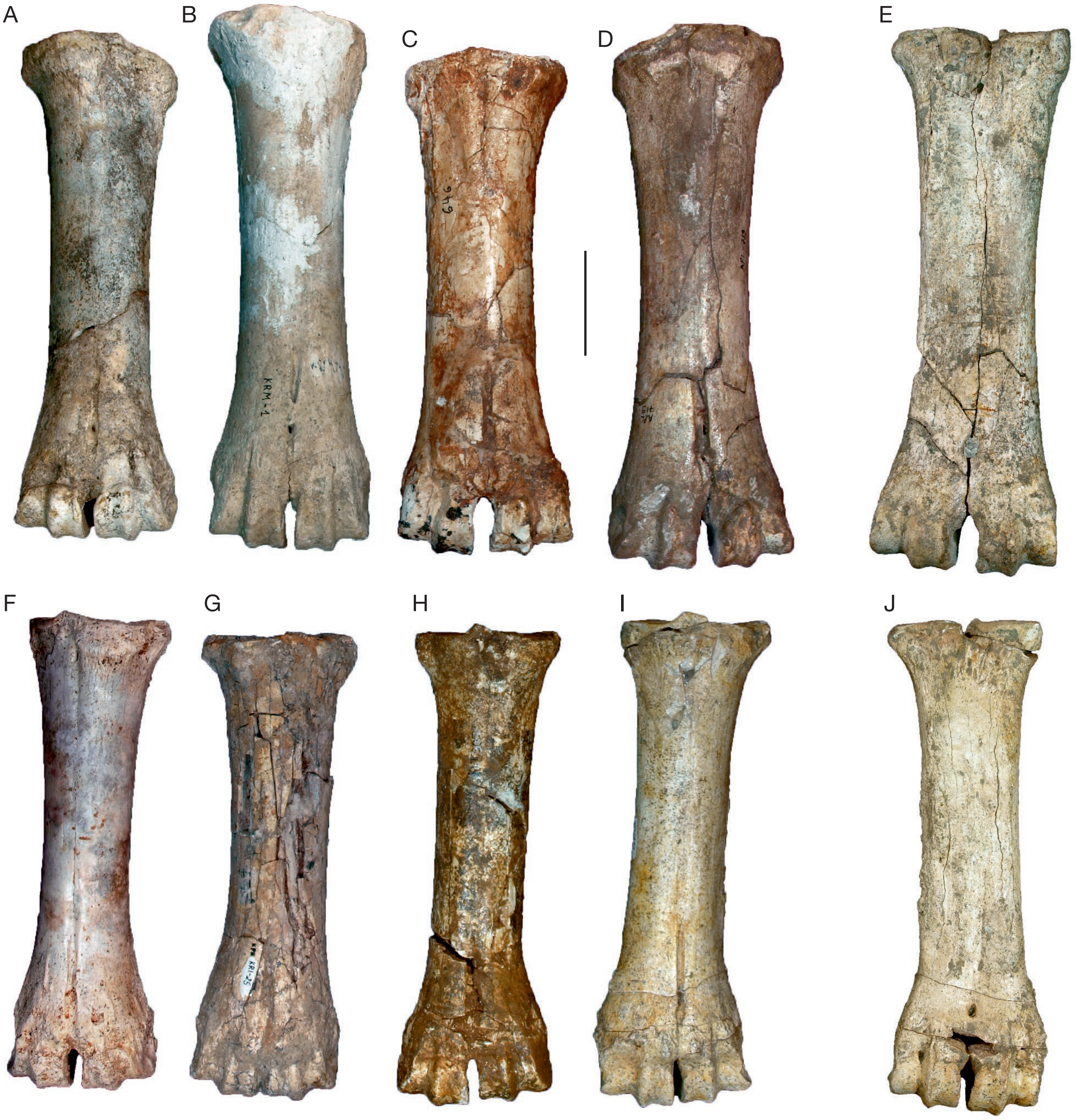

Fig. 4. — Metacarpal III+IV of *Bison* cf. *degiulii* (Masini, Palombo & Rozzi, 2013) from Mygdonia Basin, Greece: **A**-**D**, **F**-**I**, dorsal views of respectively male and female individuals; **E**, **J**, plantar views of respectively a male and a female individual; **A**, TSR D18-42; **B**, KRM-1; **C**, KLT-646; **D**, **E**, APL-719; **F**, TSR F18-55d; **G**, KRI-25; **H**, KLT-305; **I**, **J**, APL-373. Scale bar: 5 cm.

well above the base of the crown. The p3 is very similar to the p4 but with a thinner metaconid and a clear premetacristid. The partially preserved p2 (KLT-318) shows a strong entostylid perpendicular to the mesiodistal axis of the tooth and a very narrow and acute hypoconid directed distobuccally.

Metapodials

Only two metacarpals and one proximally preserved metatarsal can safely be identified as a bison (Fig. 4C, H). Both metacarpals show the typical characters of the genus: they are relatively short with broad proximal and especially distal epiphysis; "kinked" transition from distal diaphysis to distal epiphysis; isosceles triangular hamatum (unciform) facet, narrower than the magnum-trapezoid one; strongly curved dorso-medial outline of magnum-trapezoid; and moderate to strong medial tubercle of the palmar side of the proximal epiphysis laterally surrounded by a well-defined depression (Olsen 1960; Brugal 1985; Sala 1987; Gee 1993). KLT-646 is 7% longer than KLT-305 and the transition from diaphysis to distal epiphysis is smoother (less "kinked") recalling differences between respectively male and female metacarpals of the Apollonia bison (see below and Fig. 4). Both metacarpal specimens show weak distal trochlear condyle splaying (for a definition see Maniakas & Kostopoulos 2017a). Though distally severely crashed, the metatarsal (KLT-345) appears slightly longer than KLT-305 and with well-"kinked" transition from diaphysis to distal epiphysis. The cubonavicular facet of the proximal epiphysis is confluent with the facet for the large cuneiform as in bisons (Sala 1987; Gee 1993 and ref. therein). Metapodial measurements are given in Appendix 3C and 3D.

The Tsiotra Vryssi (TSR) sample

STUDIED MATERIAL. — Palate, TSR-161; left upper toothrow with P3-M2, TSR-D17-7; left M1(part)-M3, TSR-D20-10; left upper toothrow with P4-M3, TSR-E21-45; right lower toothrow with p2-m3, TSR-F20-16; left lower toothrow with p4-m3, TSR-D20-8; right m3, TSR-E19-27; left m2, TSR-E19-26; right m1, TSR-E18-13; left metacarpal III+IV, TSR-D18-42, TSR-E17-24; right metacarpal III+IV, TSR-F18-55d (part of a complete anterior foot).

DESCRIPTION

Palate TSR-161

Few morphological features may actually be extracted from the largely destroyed and weakly deformed rostral part of the cranium TSR-161 bearing both toothrows (Fig. 5). The specimen corresponds to a more than 42 months individual of European bison (Wegrzyn & Serwatka 1984) and in between S1/S2 stages (early maturity) of American bison (Skinner & Kaisen 1946), likely having an EBEA of 3 to 5 years. The staphylion opens more than 10 mm behind M3 and more caudally than the lateral palatine indentations (Fig. 5B), whose anterior edge is just at the level of M3's hypoconid. The infraorbital foramen is large (minimum estimated height at the posterior best preserved part at about 15 mm) and rather pocketing, opening 30 mm above the P2-P3 limit (Fig. 5C). The rostral-most part of the maxillary bone and important part of the premaxillary are preserved on the left side (Fig. 5A). In lateral view, the maxillary thins significantly towards its rostral end and expands well-below the premaxillary bone, whereas the ventral surface of the premaxillary/maxillary area is placed just above the alveolar level (Fig. 5A, D). The overall configuration is quite unlike that of extant bison and wisent (Fig. 5D) and more similar to that of yak and *Leptobos etruscus* (Falconer, 1859) (Fig. 5D), rather suggesting a primitive trait. Although the dorsal part of the premaxillary is not preserved, judging from the degree it tapers upwardly, we believe it ends well-before the nasals, as in *Bison* and unlike *Leptobos* (Fig. 5D).

Dentition

The upper toothrows TSR-D20-10 and TSR-E21-45 are approximately on the same wear stage with TSR-161 (Fig. 5E) and consequently a similar EBEA of 3-5 years is estimated; TSR-D17-7 represents an old individual (S4 stage of Skinner & Kaisen 1946; EBEA: 10-14 years). The P2-M3 length ranges from 149-152 mm with the premolar row length representing 66.3-68.8% of the molar row length (n=2) (dental measurements in Appendix 3A). The molars differ from those of *Leptobos* from the same site in the relatively wider labial pillars, the stronger mesostyle, the wider and squarish hypocone, the much less expressed lingual constriction on both the hypocone and the protocone, the weaker spur on fossettes (when present) and the more centrally placed paracone along the entire height of the P4. The distal part of the unworn P4 (TSR-E21-45; Fig. 5E) shows a quite complex structure: a sharp and narrow angular projection traceable along the entire height of the tooth is present in the distolingual corner, possibly representing or analogous to an incipient hypocone. At the same position or slightly behind it, a short and sharp (distocentral) spur appears in the central fossette, directed mesially. Just after, the distolingual crista divides with the distal (external) branch contacting the metastyle and the mesial branch contacting the distolabial crista (Fig. 5E). This configuration vanishes quickly with wear apart from the distocentral spur that strengthens till mid-wear stages. A very similar structure has been seen in Apollonia, Dmanisi (Bukshianidze 2005: fig. 9), Nihowan (Teilhard de Chardin & Piveteau 1930: pl. XVI, fig. 2) and in one unworn P4 of yak (HEP-AcUT). *Bison schoetensacki* from Süssenborn (Flerov 1979) and extant bisons (Skinner & Kaisen 1946: pl. 9, fig. 1c; pl. 11, figs 2c, 3c; HEP-AcUT pers. obs.) also show a very similar pattern but with a tendency for the distal (external) branch of the distolingual crista to rest independent at the top of the crown. The overall morphology of the upper molars is fully compatible with those from Kalamoto.

Three of the preserved mandibular specimens (TSR-D20-8, Fig. 3K; TSR-E19-27; TSR-E19-26) represent individuals in full maturity (S3 stage of Skinner & Kaisen 1946; EBEA: 6-8 years) and one (TSR-F20-16; Fig. 3I, J) in late adolescence (S1 stage of Skinner & Kaisen 1946; EBEA: 4-6 years) (dental measurements are given in Appendix 3B). The premolar/molar row length ratio is estimated at about 65% (TSR-F20-16). The p2 is simple but with well-developed metaconid directed distally, strong entostylid perpendicular to the mesiodistal axis of the tooth and very narrow and acute hypoconid directed distobuccally. The little worn p3 (TSR-F20-16; Fig. 3I) has a long and mesially directed parastylid associated by a weak but distinct paraconid. The anterior valley is largely open and the metaconid is distally shifted and asymmetrically expanded mesio-distally towards the base of the crown. The entoconid and the entostylid fuse very quickly together and the hypoconid is narrow, acute and directs distobuccally. The p4 (Fig. 3I-K) is morphologically similar to the p3 but the talonid is much more developed, the metaconid is more flatten lingually and more expanded mesiodistally towards the base, closing earlier the posterior valley. The molars have a strong parastylid and a very weak metastylid (Fig. 3I-K), whereas the entostylid is strong and thick along the entire

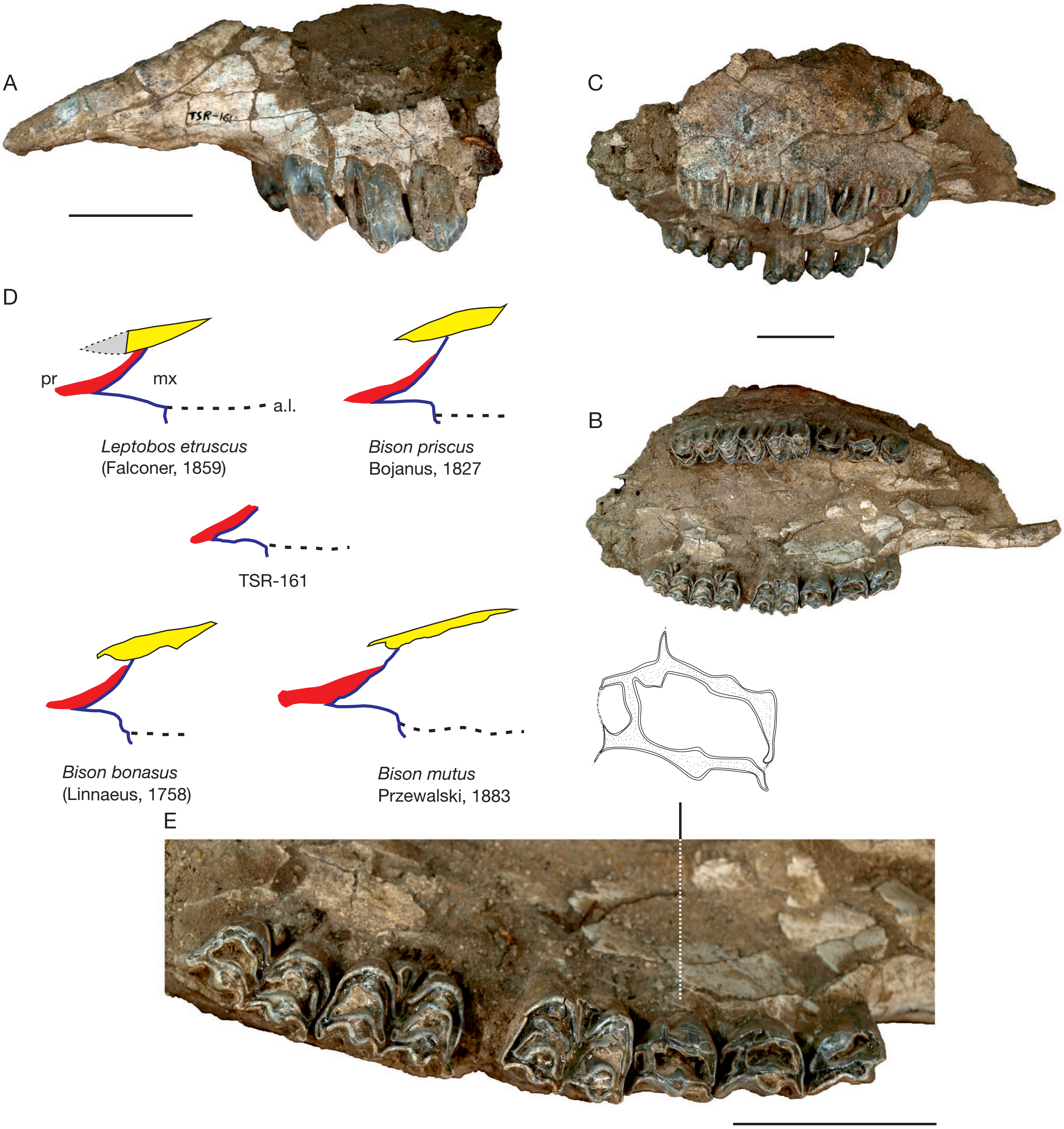

Fig. 5. — Partial cranium TSR-161 of *Bison* cf. *degiulii* (Masini, Palombo & Rozzi, 2013) from Tsiotra Vryssi, Greece: left lateral (**A**), right lateral (**B**), and palatal (**C**) views; close up of the upper left toothrow in occlusal (**E**) view and sketch of the P4 occlusal morphology (see descriptions); **D**, schematic comparison of the lateral premaxilla-nasal contact in TSR-161, *L. etruscus, B. priscus, B. bonasus* and *B. mutus*. Abbreviations: **pr**, premaxilla; **mx**, maxilla; **ns**, nasal; **a.l.**, alveolar level. Scale bars: 5 cm.

m3 height but much thinner on m1 and m2. The third lobe of m3 is semicircular shaped in occlusal view with a strong distal stylid; in moderate to advanced wear stage it appears elongated semicircular and its lingual wall is weakly curved. On the m1 and m2 the distal lobe is significantly narrower than the mesial one. The fossettes have no spurs. The unworn m1 (TSR-E18-13) with hypsodonty index at 1.7 (Table 3), exhibits in the apical part of crown a thin but acute metastylid, whereas the praeprotocristid is strongly divided forming a closed fossette on the mesial part of the tooth; the buccal branch of the praeprotocristid merges with the strong parastylid whereas the lingual branch is in contact with the praemetacristid. This configuration is lost quickly by wear and it has been seen in most unworn m1 and m2 of the Apollonia bison (see below; Fig. 3E) but it lacks from *Leptobos*.

TABLE 4. — Frequency of spurs on the fossettes of the upper molars in the early bison from Apollonia.

Frequency of:	M1 n=19-21	M2 n=14	M3 n=13
mesial spur on mesial fossette	4%	0%	19%
distal spur on mesial fossette	16.5%	14%	0%
mesial spur on distal fossette	4%	0%	0%
distal spur on distal fossette	25%	14%	62.5%

Metapodials
The three preserved metacarpals possess all morphological *Bison* features listed above. By size and proportions these specimens fit better KLT-305 and the female of the Apollonia population (see below). The distal trochlear verticilli are sub-parallel (Fig. 4A, F; Appendix 3C).

The Krimni (KRI and KRM) sample

"*Leptobos*" sp. – Kostopoulos 1996: 287-297.

STUDIED MATERIAL. — Left lower milk toothrow with dp2-m1, KRI-26; left lower toothrow with p2-p3, KRI-36; left p4, KRI-37; left m1/2, KRI-38; right m3, KRI-35; left metacarpal III+IV, KRI-25, KRM-1.

DESCRIPTION
Dentition
A left lower milk toothrow and very few isolated teeth are the only dental evidences for the presence of bison in the site of Krimni. The unworn m1 of KRI-26 bears the rather characteristic division of the praeprotocristid and the thin metastylid seen in Tsiotra Vryssi and Apollonia samples. The buccal conid of the mesial lobe of dp4 is much more crescentic than in *Leptobos* from Gerakarou site of Mygdonia Basin (specimen GER-130), whereas both ectostylids on the buccal face seem to sprout from the middle lobe, unlike *Leptobos* and similarly with the Apolonia bison. Most permanent lower teeth likely belong to a single disassembled mandible. The permanent premolars (KRI-36, 37) are relatively wider than in *Leptobos* and with stronger developed paraconid. In the single preserved and moderately worn m3 the entostylid is thick and the third lobe has an elongated semicircular occlusal outline with a strongly developed distal stylid. Measurements are given in Appendix 3B.

Metapodials
Bisons are represented in the Krimni fauna by two metacarpals (Fig. 4B, G), both exhibiting the basic features of the genus as set forth above. KRI-25 is 13% shorter than KRM-1 and shows a more pointed palmolaterally facet for the unciform and a more concave lateral profile in its lower half, recalling differences between respectively female and male metacarpals of the Apollonia bison (see below and Fig. 4). In distal view, the verticilii are almost parallel each other in KRM-1 but more diverging palmary in KRI-25. Measurements are given in Appendix 3C.

The Apollonia (APL) sample

STUDIED MATERIAL. — See Kostopoulos (1997) plus: part of the right frontal with the base of the horncore, APL-310; isolated horncore, APL-658; left upper toothrow with P2-M3, APL-746; right lower milk toothrow with dp4-m1, APL-753; left dp3, APL-756; metacarpal III+IV, APL-520 left, 578 left, 654 right, 677 left, 719 right, 738 left, 745 left; metatarsal III+IV, APL-603 right, 718 left.

DESCRIPTION
The Apollonia early bison is by far much better sampled than bisons from other sites in Mygdonia Basin, represented by 155 specimens (Number of Identified Specimens, NISP) and 20 individuals at least (Minimum Number of Individuals). Females and calves predominate over males, whereas amount of difference between the two sexes resembles that of extant *B. bonasus* and Late Pleistocene *Bison priscus* Bojanus, 1827. A detailed palaeodemographic analysis is given in Appendix 4.

Several morphological and metrical features of the bison from Apollonia site have been already presented and discussed by Kostopoulos (1997). Focus is given here on new specimens and additional features, as well as on corrected data based on the larger available sample.

Cranial material
A part of the right frontal with the base of the horncore, APL-310 originally ascribed to *Soergelia brigittae* (Kostopoulos 1997: 859), represents a young male bison individual (Fig. 6C, D). The preserved frontal bears large sinuses extended within the horncore and appear strongly swollen near the dorsal horncore base. The crown of the cornual process is more developed in the lower half of the base, whereas the contact between the pedicle and the horncore on the dorsal half is less evident. The horncore is inserted laterally and slightly curved upwards ('arched axis straight growth and straight posterior margin', following McDonald 1981). It is short (maximum estimated length at about 100 mm) and tapers fast. Its surface bears thin, shallow, irregular grooves. There is no hints of torsion. The basal cross-section is almost square-shaped with flattened ventral and strongly convex dorsal outline ('symmetrical triangular isosceles' following McDonald 1981). The basal rostrocaudal diameter (APD) is 48.0 mm and the dorsoventral one (DVD) is 56.0 mm.

An isolated possibly left horncore, APL-658 (Fig. 6A, B) belongs to a rather young and likely female individual. The horncore is detached just at the level of the crown of the cornual process and appears strongly cancellous inside. The basal cross section is ovoid with flattened ventral and strongly convex dorsal surface ('symmetrical, broadly triangular scalene', following McDonald 1981). In lateral view it appears barely curved upwards and judging from the diagonal natural section at the base compared to the longitudinal axis, it seems headed backwards. There is no torsion. The cranial surface is weakly convex and the caudal one weakly concave. The cranial and caudal surfaces are deeply grooved, as it is the basal part of the ventral surface, whereas the dorsal one is much smoother with thin, shallow irregular grooves. The complete length of the horncore might reach 200 mm (120 mm preserved). The basal craniocaudal (APD) diameter is 56.4 mm and the dorsoventral (DVD) one 47.0 mm.

Dentition
Cement is largely developed, especially between the lobes or between lobes and styles/ids, being more extensive in some specimens where it covers most of the molar's and premolar's surface; as is expected it is much thinner in young individuals than in old ones. DP2 is large compared to P2 and with much more developed anterior complex (parastyle+protocone) (Fig. 3A, B). The mesial lobe of DP3 is wider than the distal one and square shaped. The fully molariform DP4 has a strong and thick parastyle but thin meso- and metastyles (Fig. 3A, B). The hypsodonty index of permanent molars ranges from 1.3-1.6 (Table 3). The upper toothrow length (P2-M3) varies between 135.0 mm and 150.0 mm (n=3) with premolar to molar row length ratio ranging from 66.1 to 76.5% (upper teeth measurements in Appendix 3A). The entostyle represents 75% of the M2 (APL-495) and 79% of the M3's (APL-240) height. The P2 and P3 have an assymetrical occlusal outline with distobuccally projected metastyle (Fig. 3C, D; Kostopoulos 1997: fig. 8B). The parastyle is strong, especially on P3 where a weak, blunt spur occurs at the distolingual corner of the central fossette. The paracone pillar is placed close to the parastyle with its anterior wall being vertical and its posterior wall subparallel to the mesiodistal axis of the tooth. The paracone is much stronger and protrudes buccally on P2, less on P3 and much less on P4 (Fig. 3C, D; Kostopoulos 1997: fig. 8B). The last upper premolar has a more symmetrical subtriangular occlusal outline and the metastyle is well developed, still thinner than the parastyle. The morphology of the unworn P4 APL-746 is very similar to that of TSR-E21-45 described previously. Overall molar morphology is typically bovine (see also Kostopoulos, 1997: 854) matching that of previous samples of KLT and TSR (Fig. 3C, D; Kostopoulos 1997: fig. 8B). A central islet is present in one out of 24 M1 (4%), in none of the 14 M2 and in five of the 16 M3 (31%). Spurs on central fossettes of M1 and M2 are mostly observed on young individuals but they are more often and persist later in life on M3. Distal spur on the distal fossettes are more common than other ones, whereas spurs appear to be more often on M1 and M3 than on M2 (Table 4).

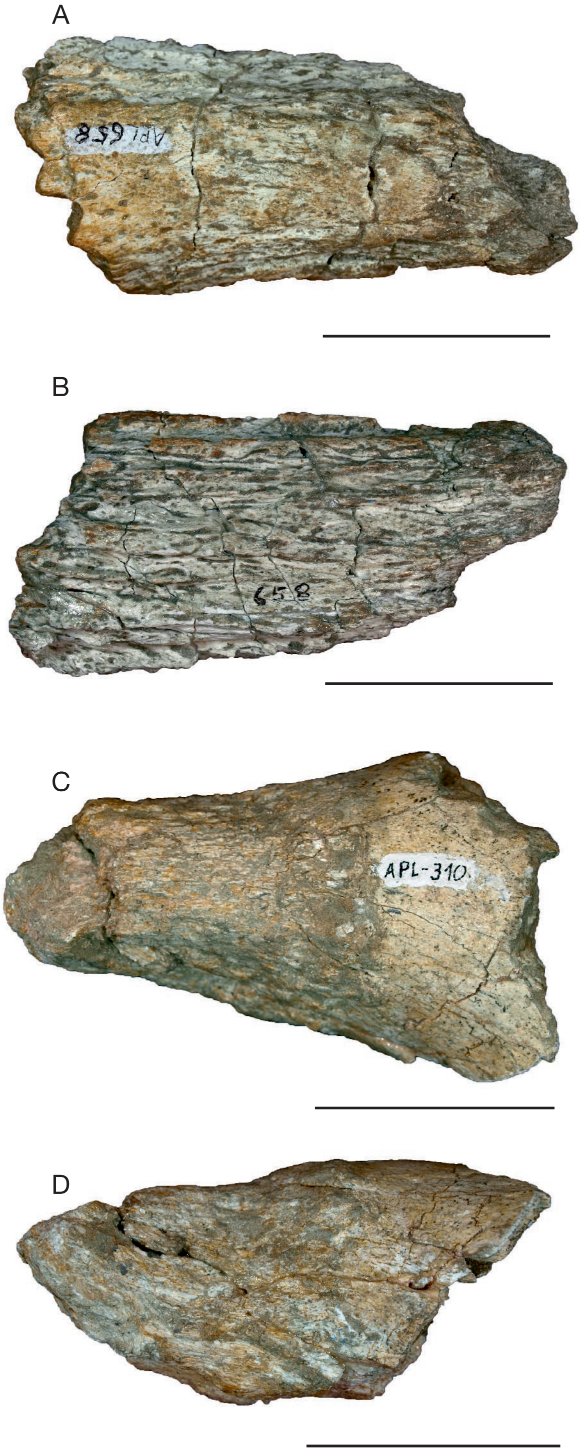

Fig. 6. — Horncores of *Bison* cf. *degiulii* (Masini, Palombo & Rozzi, 2013) from Apollonia-1, Greece: **A**, **B**, ?left basal female horncore, APL-658, dorsal (**A**) and ventral (**B**) views; **C**, **D**, right young male horncore, APL-310, dorsal (**C**) and caudal (**D**) views. Scale bars: 5 cm.

The dp3 has a much thicker paraconid than parastylid, oriented perpendicular to the mesiodistal axis of the tooth; the metaconid is short and directs always distolingually (Fig. 3E, F). The dp4 bears a strong parastylid curving distally and a thin but distinct entostylid in the upper part of the crown (Fig. 3E, F). On two out of ten deciduous toothrows the dp4 bears a lingual stylid between the second and the third lobe. On the buccal side, the ectostylids grow up from the central lobe (Fig. 3E). The lower permanent toothrow length (p2-m3) is 143.0 mm, measured on just one complete but senile specimen (APL-478; Kostopoulos 1997: fig. 8A) with premolar to molar length ratio at 57.5%. Teeth measurements are given in Appendix 3B. The p2 is simple but with well-developed metaconid directed distolingually. On the p3 the paraconid is weak but distinct, the anterior valley closes near the base of the tooth, the entostylid fuses with the entoconid from the very initial wear stages and a very narrow hypoconid appears on the distobuccal corner, separated from the protoconid by a narrow and deep groove. The p4 is very similar to the p3 but the parastylid is much thinner and the paraconid more clearly developed having a perpendicular orientation compared to the mesiodistal axis of the tooth or leaning slightly backwards. The metaconid of the p4 is more mesiodistally expanded especially towards the base, where

FIG. 7. — Metatarsals III+IV of *Bison* cf. *degiulii* (Masini, Palombo & Rozzi, 2013) from Apollonia, Greece, dorsal views of: **A**, right, female metatarsal, APL-192; **B**, right, female metatarsal, APL-97; **C**, left, male metatarsal, APL-66; **D**, left, male metatarsal, APL-194. Scale bar: 5 cm.

tends to be fused with the talonid leaving open the anterior valley; still the posterior valley rests as a shallow fissure till the base of the crown. On seven m1 at initial stage of wear the praeprotocristid is bifurcated forming a closed fossette on the mesial part of the tooth; the buccal branch of the praeprotocristid merges with the strong parastylid whereas the lingual branch is in contact with the praemetacristid (Fig. 3I). The lower molars, especially the m3, have a strong parastylid and columnar-like lingual pillars. The lingual valley between the metaconid and the entoconid has an open-U profile at initial wear stages but tends to be flatten with wear. The entostylid is weak on m1, and m2 but well distinct on m3, especially on less worn specimens. An ectostylid appears only between the first (mesial) and the second (intermediate) lobe of m3. The third lobe of m3 has an elongated semicircular occlusal outline with a distinct distolingual stylid; in advanced wear stages the occlusal outline becomes roughly rounded.

Metapodials

Morphological features of both metacaprals (Fig. 4D, E, I, J) and metatarsals (Fig. 7) fit pretty well those referred to bisons, e.g. broad proximal and especially distal epiphysis compared to diaphysis; "kinked" transition from distal diaphysis to distal epiphysis; triangular shaped hamatum facet, narrower than magnum trapezoid one and strongly curved rostro-medial outline of the magnum-trapezoid facet on metacarpals; dorsal vascular groove visible only on the proximal ¼ and distal ⅓ of the metacarpal's length; confluent anteriorly facets for the cubonavicular and large cuneiform of metatarsals; frequent presence of a small tubercle on the

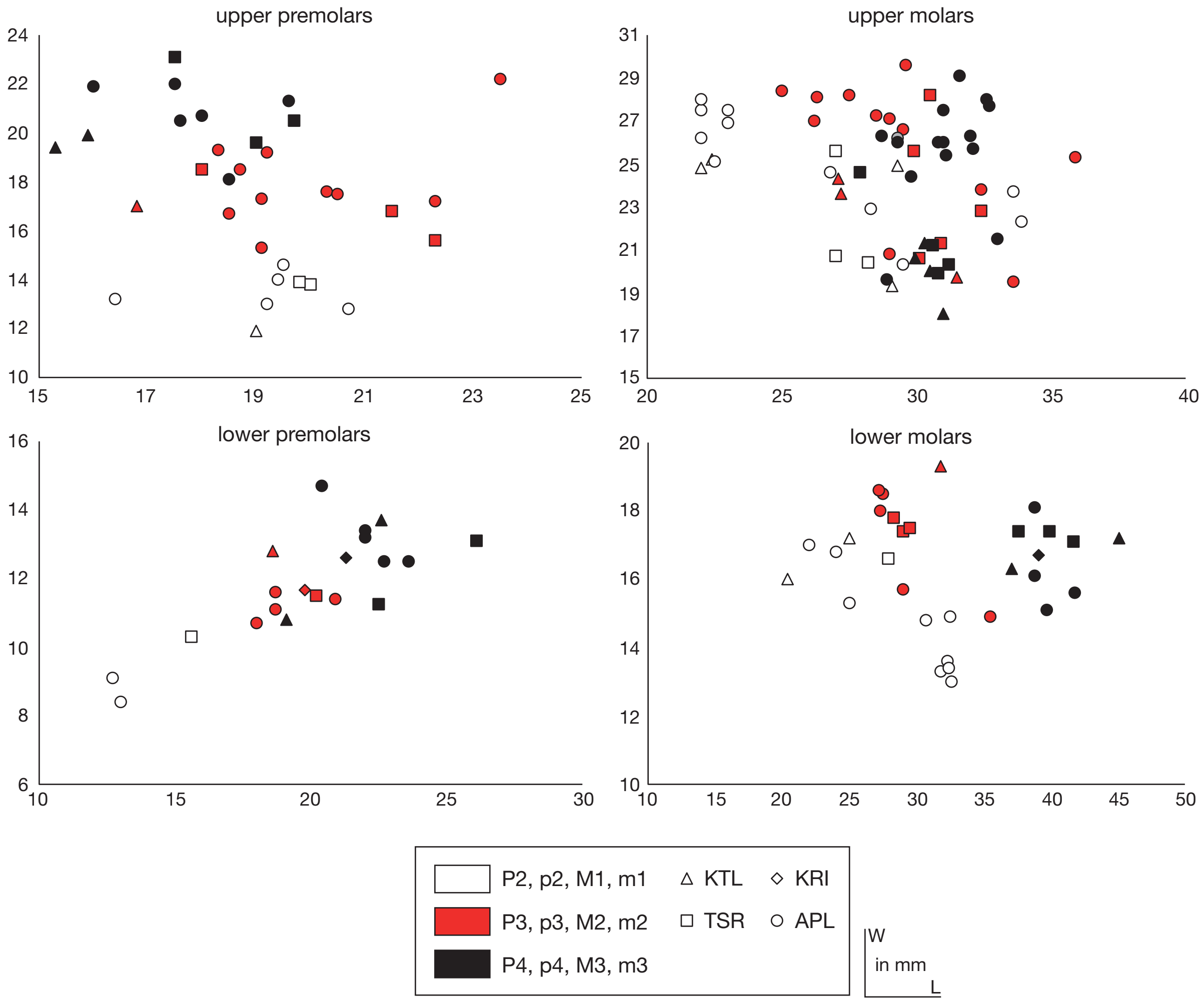

FIG. 8. — Bivariate diagram (length [L] against width [W]) comparing the bison upper and lower teeth proportions from the Mygdonia Basin. Abbreviations: **APL**, Apollonia-1; **TSR**, Tsiotra Vryssi; **KLT**, Kalamoto-2; **KRI/KRM**, Krimni.

palmomedial corner of the facet for the large cuneiform on metatarsals (Sala 1987; Gee 1993 and ref. therein). Both metacarpals and metatarsals show increased distal trochlear condyle splaying (see Maniakas & Kostopoulos 2017a) (Figs 4D, E, I, J; 7).

A residual articular surface for the fifth metacarpal is present in six out of 17 metacarpals (35.3%; Fig. 4E, J) whereas the remains of the fusion of the second metacarpal (seen usually as an elongated crest on the palmomedial corner of the third metacarpal) is present in eight out of 17 specimens (47%; Fig. 4E, J); in both cases the character is more frequent in females than in males (57 vs 50% in the first case and 54.4 vs 33% in the second). Supplementary bony growths are seen in very few adult specimens of both sexes, usually restricted in the area below the distal dorsal canal and the condyles and/or along the lateral margins of the shaft (Fig. 4I, J). Males, usually exhibit a relatively larger dorsomedial tuberosity for the extensor radial muscle of the wrist, almost double-sized palmar distal canal and significantly more rough lateral edges along the upper half of the plantar surface (Fig. 4D, E, I, J).

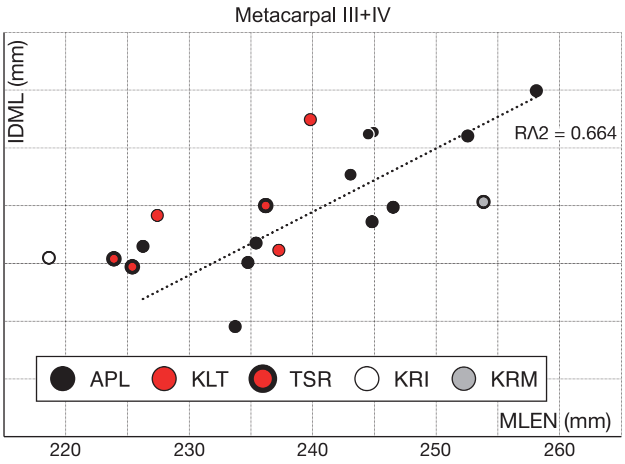

FIG. 9. — Bivariate diagram of the bison metacarpal III+IV proportions (length [**MLEN**] against distal width [**IDML**]) from the Mygdonia Basin. Abbreviations: **APL**, Apollonia-1; **TSR**, Tsiotra Vryssi; **KLT**, Kalamoto-2; **KRI/KRM**, Krimni; **R²**, Pearson coefficient. The dotted line represents linear regression of the APL sample.

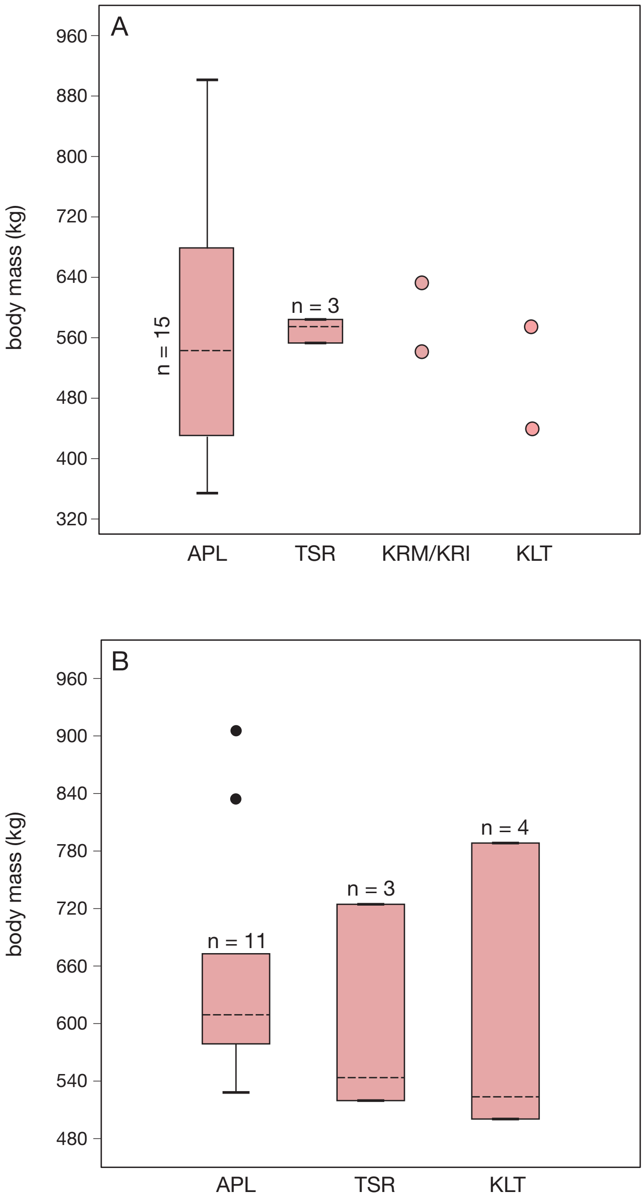

FIG. 10. — Box plots of the body mass (in kg) variation of the local samples of bisons from Mygdonia Basin, based on estimations from (**A**) the metacarpal III+IV (see Material & Methods) and (**B**) the M1 occlusal area (following estimation equation by Legendre 1986). Abbreviations: **APL**, Apollonia-1; **TSR**, Tsiotra Vryssi; **KLT**, Kalamoto-2; **KRI/KRM**, Krimni. For a detailed weight analysis according to age and sex of the Apollonia population see Appendix 4.

COMPARISON

Among diachronous Mygdonia bison populations

KLT, TSR, KRI/KRM and APL cover a timespan from approximately 1.7 Ma to 1.2 Ma (Fig. 1; see also Konidaris *et al.* 2015). Comparison of the biometrical and morphological features of the bison populations from these sites is feasible only among dental and postcranial remains (here restricted to metacarpals, as complete metatarsals are only known form APL), which point to the presence of a single species (Figs 8; 9). Small differences between specimens from different sites appear meaningless when apply criteria of wear stage, ontogenetic age or sexual bimodality, while others are of minor importance in the light of the known intraspecific variability of extant species; in most cases differences among samples do not exceed intrapopulation variability seen in the best documented APL sample (Figs 8; 9). Some other differences may, however, due to the local evolution and adaptations of the Mygdonia population through time. Thus, dentitions from TSR, KRI and KLT show, less developed cement around the teeth than the APL bison, though samples from the former sites are rather limited for definitive conclusions. On the other hand, the small metacarpal sample from TSR indicates slightly smaller proportions at the average (Fig. 9) than the bisons from the rest sites, while the distal trochlear condyle splaying of the metacarpals apparently increases from TSR to APL.

Estimated body mass based on metacarpals (ABME) gives a range of 553.1-584.3 kg for the three individuals from Tsiotra Vryssi, 541.7 kg for the single female of KRI and 632.8 kg for the single male of KRM, 439.9 kg for the single female and 575.3 kg for the single male of KTL, all values well within the estimated ranges for the APL bison (Fig. 10A). Body mass estimation based on M1 area (Fig. 10B based on equation by Legendre, 1986) gave at average 650 kg for APL (n=11), 584 kg for KLT (n=4) and 595 kg for TSR (n=3); Kruskall-Wallis test shows no significant differences between pairs (APL-TSR, APL-KLT or TSR-KLT).

With other Eurasian Early-Middle Pleistocene bisons

A comparison of basic cranial features (corrected for the size effect, following Mosiman's transformation) among known fossil crania of early bisons and those of *B. bonasus* reveals that variability in proportions (shape) of extinct forms exceeds largely that seen in a single extant species (Fig. 11). Thus, *B. bonasus* crania are cluster closely together independently of age and sex whereas those of fossil taxa distribute largely on the morphospace. PC1 axis (accounted for *c.* 40% of the total variance) mainly divided crania with large minimum distance between temporal fossae and widely separated supraorbital foramina on frontals at the positive end from those with widely separated horncores (expressed here as the distance between the back edges of the horncore bases) and less constricted postorbitally at the negative end. On that ground, *B. bonasus* and KLT crania are placed diametrically opposite to those of *L. etruscus* and *B.* (*E.*) *palaeosinensis* Teilhard de Chardin & Piveteau, 1930, the latter having a between-horncore distance of 275 mm, i.e., significantly larger than in other studied early bison crania (< 200 mm).

Examined crania are further grouped into distinct units at the morphospace level defined by the second and the third principal components of variation accounted for 23% and 20% of total variance, respectively (Fig. 11). Hence, Crâne A from Nihowan and the Dmanisi cranium occupy the positive end of PC2, which mainly expresses high loadings of bimastoid width, large distance between the supraorbital foramina, and weak postorbital constrictions, whereas the crania from KLT and Pirro Nord occupy the positive end of PC3, which mainly expresses high loadings of frontal length and biorbital width.

Horncore absolute size and proportions vary greatly within Mid-Late Pleistocene European *Bison* (Fig. 12), being greatly

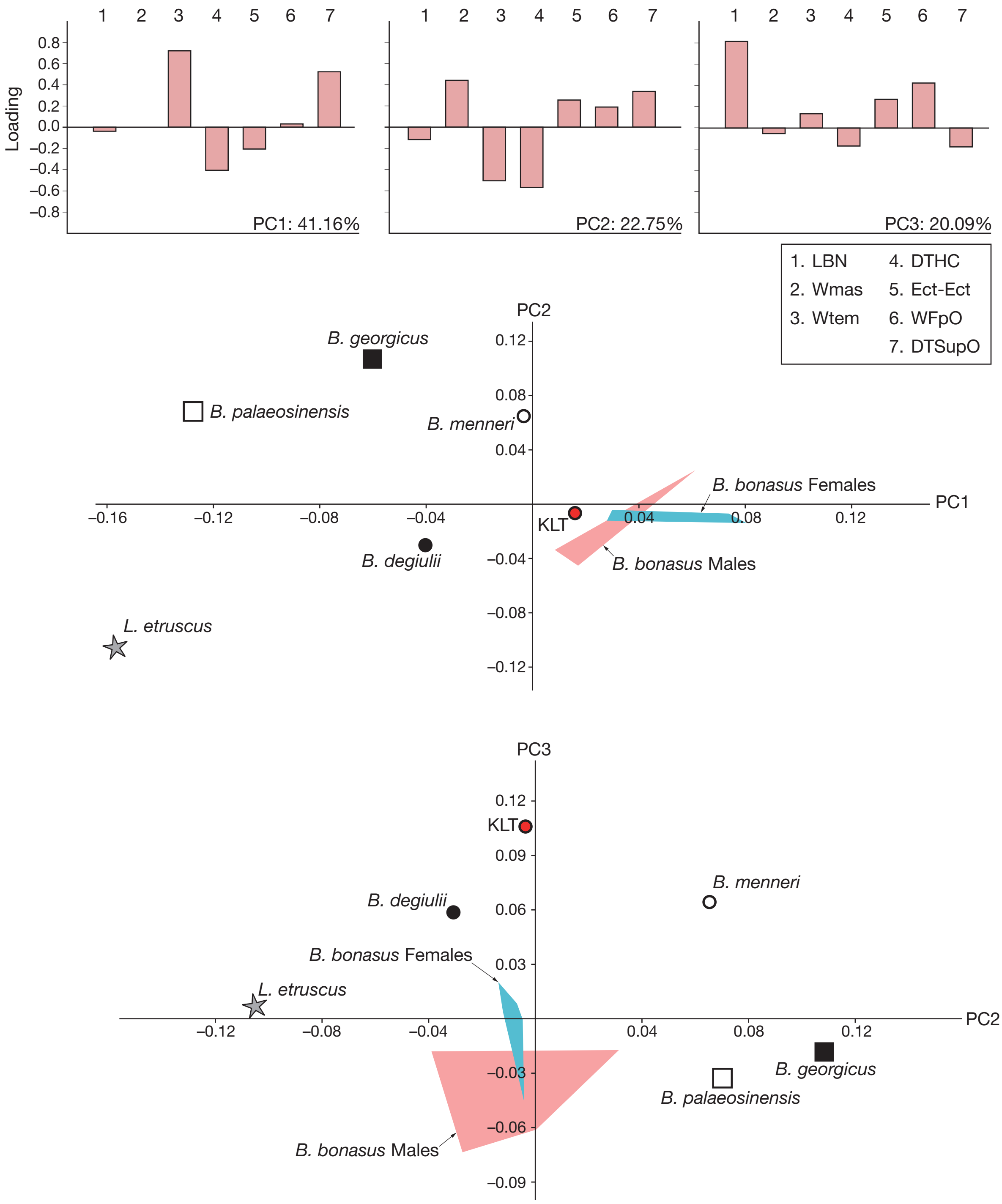

FIG. 11. — Principal component analysis (PCA) of seven basic cranial features (corrected for the size effect, following Mosimann's transformation, see Material and methods) among known fossil crania of early bisons and those of *B. bonasus* (4 males and 5 females; **shaded areas**). Principal component (**PC**) loadings and percentage of total variance accounting for the first three axes are given in the histograms at the top. PC1-PC2 plan is given in the upper graph and PC2-PC3 in the lower. Abbreviation: **KLT**, Kalamoto-2 cranium (KLT-638). Abbreviations of cranial linear measurements as in Table 2.

exaggerated by sexual dimorphism. All early bisons show smaller horncores compared to those of *B. schoetensacki* Freudenberg, 1910 and *B. priscus*, with the largest and likely male specimens of *B.* (*E.*) *palaeosinensis* (Crâne A), *B.* (*E.*) *georgicus* and the holotype of *B. tamanensis* Vereshchagin, 1959 being placed close to those of large leptobovines and within the range of the smaller (female) specimens of *B. schoetensacki* from Isernia la Pineta and Mauer (Fig. 12). The likely female cranium from KLT displays even smaller horncores as it might be expected but the same is also true for the Pirro Nord cranium which most possibly represents a male. The young male horncore APL-310 appears proportionally similar to young male individuals from Dmanisi and Untermassfeld referred to *B.* (*E.*) *georgicus* and *B. menneri* respectively (Fig. 12).

Table 5. — Comparison of several morphometrical bison cranial features (data from Teilhard de Chardin & Piveteau 1930; Skinner & Kaisen 1946; Empel 1962; Sala 1987; Masini 1989; Sher 1997; Bukshianidze 2005; Kobryńczuk *et al.* 2008; Vasiliev 2008; Tong *et al.* 2016 and personal data). Abbreviations: **y**, young individual; **est**, estimated from published illustrations; **F**, females; **M**, males.

	KLT	***B.* (*E.*) *palaeosinensis* Teilhard de Chardin & Piveteau, 1930**	***B.* (*E.*) *georgicus* (Burchak-Abramovich & Vekua, 1994)**	***B. menneri* Sher, 1997**	***B. degiulii* (Masini, Palombo & Rozzi, 2013)**	***B. schoetensacki* Freudenberg, 1910**	***B. priscus* Bojanus, 1827**	***B. bonasus* (Linnaeus, 1758)**	***B. bison* (Linnaeus, 1758)**
Frontoparietal angle	100	99	90 (I measure 115)	85y-95 (est)	*c.* 90	87 (n=1)	< 90	≤ 90	≤ 90
Horncore-sag.pl. angle	60	69	65	≥ 55	65	65-92 (n=8)	60-85	60-80 (n > 10)	70, 73, 75
Sincipital-Occipital angle of Frontals	146	–	135-140	*c.* 140-150	140	140-155	160-165	–	–
LNB/WFpO	*c.* 1.09	*c.* 0.82 (est)	0.92	*c.* 1.1 (est)	0.96	1.0-1.1 (n=2)	0.93	–	0.87-1.1 (n=5)
LNB/WFpO	< 0.29	< 25 (est)	< 25 (est)	< 35 (est)	27 (est)	–	< 35	< 35	
LNB/Ect-Ect	0.72	–	0.6	*c.* 0.65 (est)	0.7	–	0.58	0.56-0.72 (n=4)	0.57-0.63 (n=4)
Wtem/WFpO	55	< 50	0.4 (est)	45-50 (est)	52	–	56-77	F: 0.57-0.64 (n=3) M: 0.59-0.69 (n=4)	–
LNB/WFpO	0.86	0.63 (est)	0.6	0.75 (est)	0.7	–	0.63	F: 0.96-M:0.89 (n=2)	F: 0.73-0.8 (n=3) M:0.65-0.7 (n=4)
Orbital Tubularity	no-weak	? weak	weak	no	weak	moderate	strong	strong	strong
Occipital outline	symmetrical pentagonal	asymmetrical pentagonal	symmetrical pentagonal	high semicircular (est)	dorsoventrally compressed trapezoid	dorsoventrally compressed semicircular	asymmetrical pentagonal	squarish	short semicircular-pentagonal
Dorsal occipital acme (a) vs dorsolateral occipital acme (b)	a ≥ b	a < b	a ≥ b	?	a >> b	a < b	a < b	a > b	a > b
Occipital max Height/ Wmas	1.66	1.6 (est)	1.6 (est)	*c.* 1.20-1.4 (est)	2.1 (est)	1.6 -1.75 (est)	1.75-1.85 (est)	F: 1.5; M: 1.4	F: 1.5-1.7; M: 1.6
Pedicles long/short	short	long	long	short	short	short	short	short	short
Pedicles bending down/up	weakly bent down	horizontal to weakly bent down	weakly turn up	weakly turn up	weakly bent down	horizontal to weakly bent down	horizontal to bent down	horizontal to bent down	horizontal to bent down
DTSupO /LNB	0.69	0.9 (est)	0.86	*c.* 0.85	0.69	–	*c.* 1	–	0.9-1.0 (n=6)
LpOaHC /LNB	0.34	0.5 (est)	0.4 (est)	0.45 (est)	0.33	–	0.46	–	F: 0.46-0.53 (n=3) M:0.45-0.53 (n=3)
Ventral level of horn-cores compared to occipital passes from:	upper third of occiput	upper third of occiput	upper third of occiput	?	upper third of occiput	top of occipital condyles	top occipital condyles	upper third of occiput	upper third of occiput

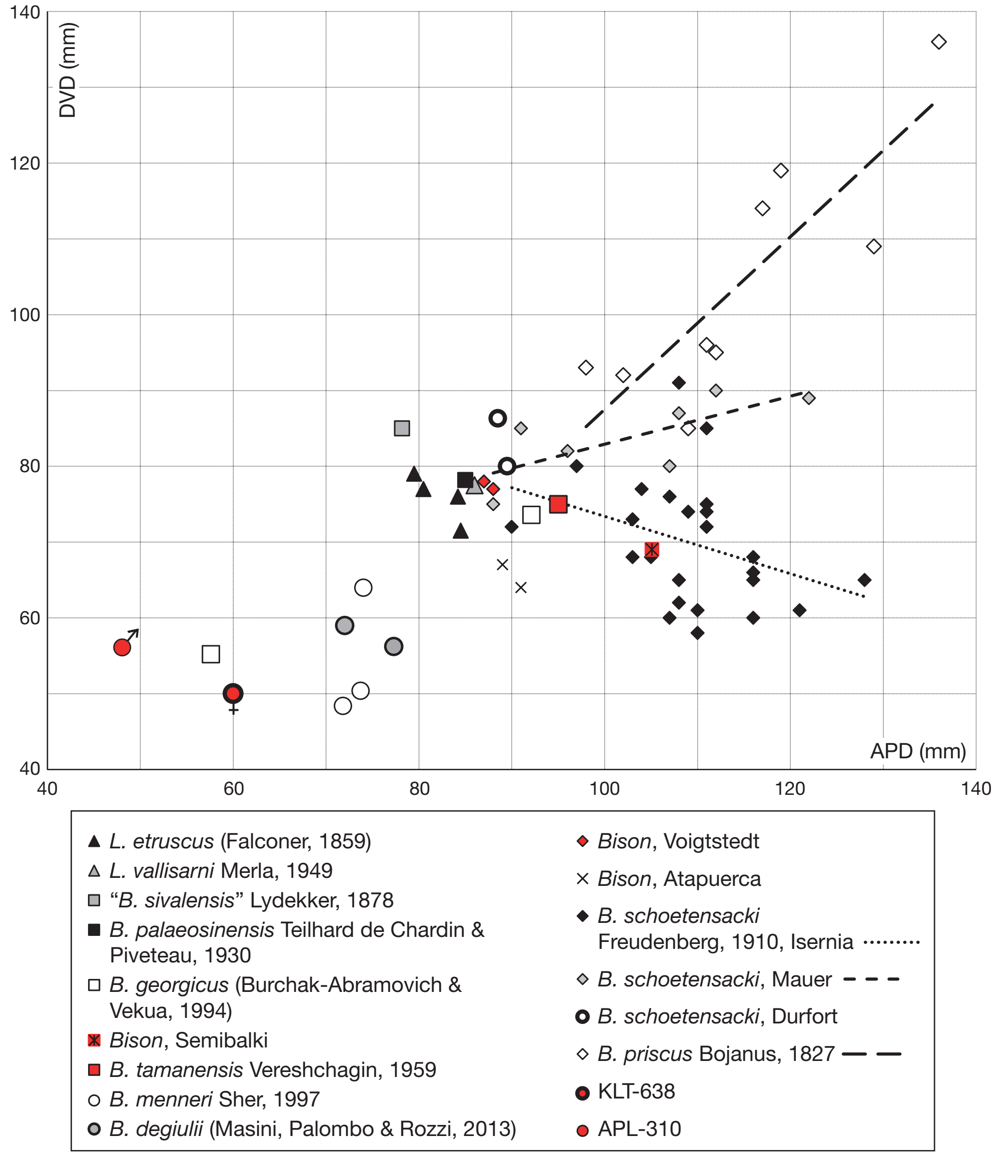

FIG. 12. — Bivariate diagram of basal horncore proportions [rostrocaudal (**APD**) against dorsoventral (**DVD**) diameter] comparing several European *Leptobos* Rütimeyer, 1877-1878 and *Bison* Hamilton Smith, 1827 samples and species. **Dashed lines** represent regressions of *B. schoetensacki* (Isernia la Pineta and Mauer) and *B. priscus*.

Flerov (1979), Sala (1987), Sher (1997) and Bukshianidze (2005) discuss a set of morphometric changes in bison crania during their evolution. A review of most of these characters indicates that several changes do not follow a linear trend from a less to a more derived condition, whereas others do not really discriminate between early and later or extant taxa (Table 5).

The divergence angle between the horncore axis and the sagittal plane is supposed to increase towards recent. All early bisons examined here gave values between 55° and 70°, which, however, are within the range of either *Bison* from Isernia la Pineta, Italy and Voigtstedt, Germany (60-92°; n=8) or extant bisons (60-80°; n>10, according to Sher 1997) (Table 5). The same is true for the relation between the length of the opisthocranium (inion-nasion chord: LNB) relative to the minimum cranial width at the postorbital constrictions (: Ect-Ect) ranging from 0.82 to 1.19 in early crania and 0.87-1.1 (n=5) in *B. bison* (Table 5). As in the Late Pleistocene and extant bisons, early taxa show similarly shortened parietals and frontals (Table 5). KLT, and Pirro Nord crania show relatively longer frontals (LNB/WFpO: 0.86 and 0.70, respectively) than the Dmanisi and Crâne A from Nihowan (0.60 and 0.63, respectively) but again differences are of the magnitude of sexual dimorphism in *B. bison* (Table 5). In all early forms, the level defined by the ventral surfaces of the horncores (in caudal view) passes through the upper half of the occipital area and rather close to the ventral end of the occipital protuberance. A similar condition is seen on crania of *B. bison* (Skinner & Kaisen 1946: pls 9, 10) whereas in the bisons from Isernia la Pineta and Voigtstedt and in the much heavier *B. priscus,* the same level reaches the top of the occipital condyles.

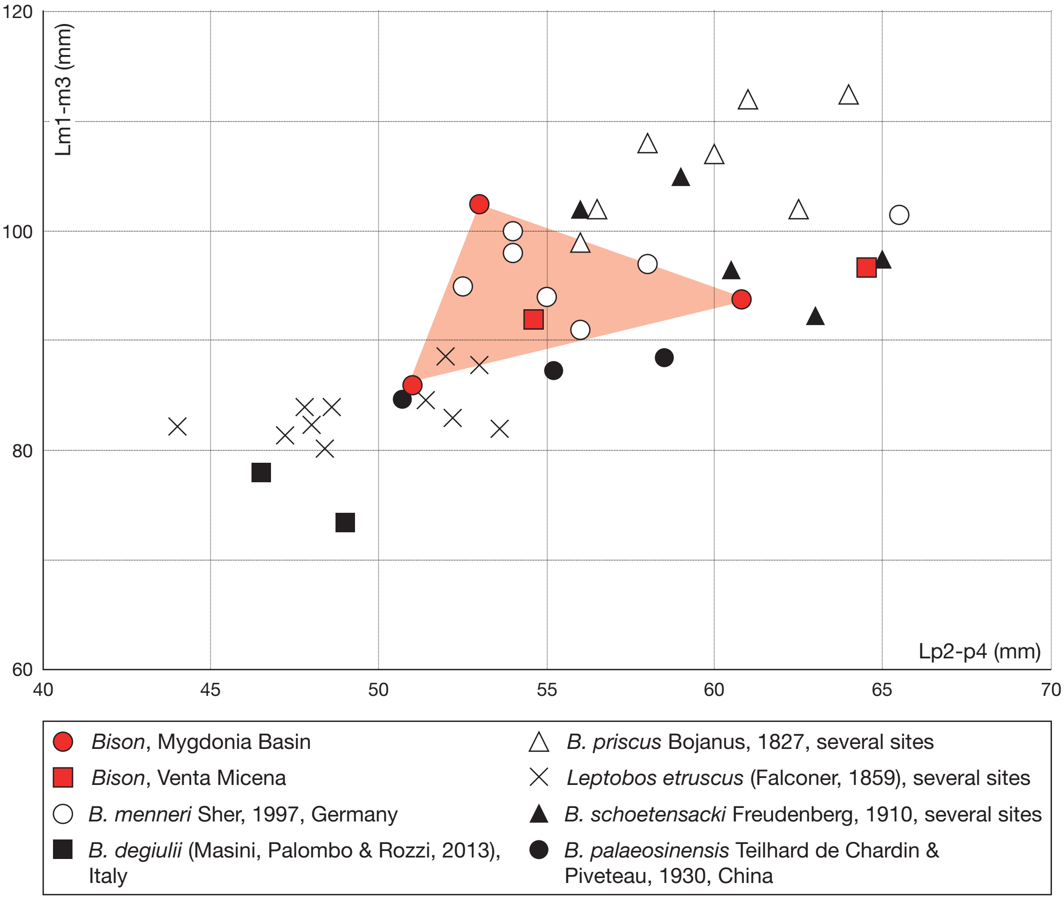

FIG. 13. — Bivariate diagram of lower teeth segments (length of the premolar row against length of the molar row), comparing several European *Leptobos* Rütimeyer, 1877-1878 and *Bison* Hamilton Smith, 1827 samples and species.

In extant bisons, as well as in *B. schoetensacki* and *B. priscus* the frontoparietal angle (formed by the coronal sutures) is less than or equal to 90° but all early crania give slightly larger values between 90-115° (Table 5), which may indeed be interpreted as a less derived feature. The angle between the sincipital and occipital faces of the frontals ranges from 135° to 150° in early crania (Table 5), similar to that of *B. schoetensacki* (140-155° according to Sala 1987) and smaller than in *B. priscus* (160-165° according to Sala 1987). Tubularity of eye sockets certainly increases through time with all early crania showing no to weakly tubular orbits; *B. priscus* and extant bisons have strongly tubular orbits (especially the males), whereas *B. schoetensacki* presents an intermediate condition. Pedicles are short in all later and extant taxa, as well as in the KLT specimen, the young Untermassfeld frontlet (IQW 1980/17380) and the Pirro Nord cranium; conversely the Dmanisi and Nihowan crania show primitively long pedicles (Table 5). Additionally in all examined forms, pedicles are settled horizontally or slightly bent down except of the Dmanisi and possibly Untermasfeld crania, in which pedicles slightly rise above the frontal level. Nevertheless, ontogeny and sexual dimorphism appears to strongly affect this feature. KLT and Pirro Nord crania also share less widened frontals at the level of the supraorbital foramina (DTSupO/LNB: 0.69 at both) than the Crâne A from Nihowan, and the Dmanisi cranium, which appear to have reach already the condition seen in *B. priscus* and *B. bison* (Table 5). The posterior shift of the horncore relatively to the orbit (i.e., the chord from the posterior margin of orbits to the anterior margin of the horncore base: LpOaHC) is always about half of the frontal length (Table 5) except again in the Pirro Nord and KLT crania where horncores and orbits set closer each other (Table 5). As mentioned by previous authors, the shape of the occipital face is related to the dorsocaudal extension of the temporal fossae and the degree of their caudal convergence. Convergence between the dorsocaudal margins of the temporal fossae is more accentuated in Crâne A from Nihowan and the Dmanisi cranium (Wtem against to the minimum width of skull at the postorbital constrictions, WFpO ≤ 50%) than in *B. priscus* (56-77%) or *B. bonasus* (57-69%; n=9) (Sher 1997). KLT and Pirro Nord crania show an intermediate condition (50-55%; Table 5), whereas bisons from Isernia la Pineta and Voigtstedt appear already as derived as priscoid and extant bisons (Table 5). Among early bison crania, the likely male Pirro Nord one shows the most wide and low occipital face (index bimastoid width, Wmas against total occipital height: 2.1) with a long and flattened to weakly concave dorsal acme and shorter, concave dorsolateral ones. KLT, Dmanisi and *B. bison* crania approach this condition being, however, less extended transversally (same index approx. 1.6; Table 5); *B. bonasus* occipital face is also similar but even

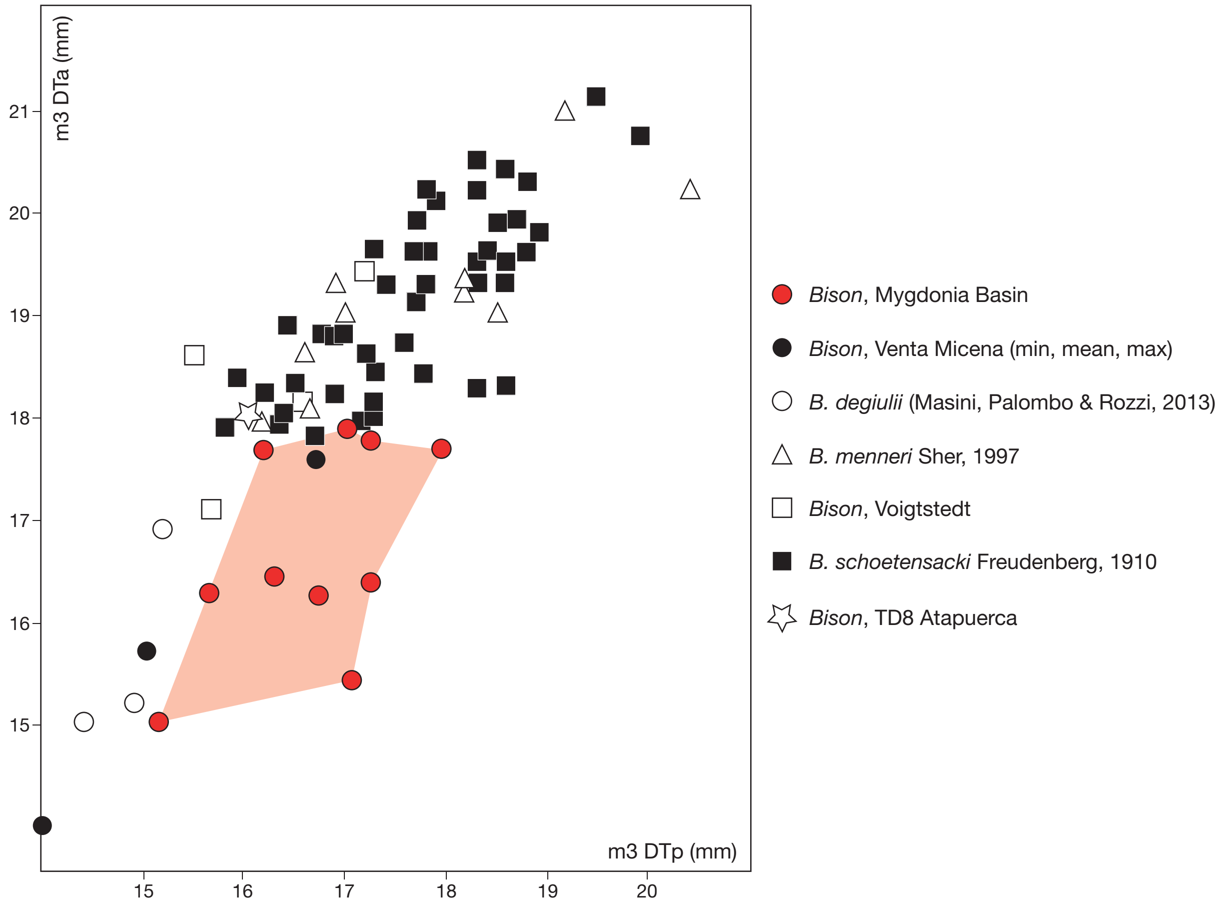

FIG. 14. — Bivariate diagram of the width of the posterior (**DTp**) and anterior (**DTa**) lobe of the m3, comparing several European *Bison* Hamilton Smith, 1827 samples and species (modified from Made *et al.* 2017). *Bison schoetensacki* Freudenberg, 1910 sample includes m3s from Mauer and Süssenborn, Germany.

less widened (same index 1.4-1.5). On the other hand, the proportions of the occipital face of the Crâne A from Nihowan are similar to those from Dmanisi (same index appx. 1.6) but the dorsal acme is much shorter than the dorsolateral ones. Such a configuration reappears on bison crania from Isernia la Pineta and Voigtstedt, as well as on *B. priscus* but widening slightly increases and the overall profile tends to be more convex (semicircular).

B. tamanensis partial holotype cranium (ZIN 26010/1) appears more derived than *B.* (*E.*) *palaeosinensis* and *B.* (*E.*) *georgicus* (Burchak-Abramovich & Vekua, 1994) in the more laterally inserted horncores and shorter pedicles, though the pedicle and basal part of the horncore are set here more horizontally. The temporal fossae approach each other less than in the Dmanisi and more than in the Pirro Nord and KLT crania, resembling closer the Nihowan condition. The occipital shape with a long concave dorso-lateral acme of the nuchal crest also resembles better *B.* (*E.*) *palaeosinensis* than Dmanisi, Pirro Nord or KLT bisons. It also differs from the latter two specimens in the much longer postcornual part of the cranium and from the Pirro Nord male cranium in the less bending down pedicles.

The cranial anatomy of the Venta Micena bison is barely known through a badly preserved frontlet (VM 8000) illustrated but not described by Martínez-Navarro *et al.* (2011: fig. 4). The specimen most likely represents a female individual that did not yet reach maturity (small distinctly grooved and slightly twisted horncores, absence of pronounced dorsally crown of the cornual process, distinctly open frontal suture, very small size). The frontals are significantly wide and flat between the horncores, the pedicles are very short and set at the frontal level, and the horncores are laterally-posterolaterally inserted and very openly curving upwards. By those features it resembles closer the KLT cranium than other crania examined here, whereas the basal dimensions of the horncore are comparable to those of the female horncore APL-658. Nevertheless, the immature state of the Venta Micena frontlet cannot provide safe conclusions.

Dental metrical data are rather scarce to be fully compared. The Mygdonia bison shows similar ranges of upper and lower toothrow segments (LPM, LP, LM, Lpm, Lp, Lm) to *B.* (*E.*) *palaeosinesis, B. menneri* Sher, 1997 and the Venta Micena bison (Fig. 13). For a larger cranium, *L. etruscus* displays smaller toothrows at the average but similarly short premolar row compared to the molar one. *B. degiulii* has a surprisingly smaller dentition, whereas dentitions referred to *B. schoetensacki* are slightly larger at the average (Fig. 13).

According to the graphical data provided by van der Made (1999: fig. 17) the proportions (maximum length against maximum width) of the p2 of the Mygdonia bison range from the largest known values for the Pirro Nord bison and the mean of Venta Micena to the smaller from Mosbach, overlapping strongly with the p2 of bison from Isernia la Pineta and Voigtstedt. Conversely, the lengths of the p3 and the p4 of the Mygdonia bison show ranges in between those of Pirro Nord/Venta Micena and the Voigtstedt bison, being shorter than the same teeth from Irernia la Pineta and Mosbach. Concerning the m3 proportions (width of the posterior against width of the anterior lobe; comparison based on van der Made *et al.* 2017: fig. 17; Fig. 14), the Mygdonia bison has similar width of the anterior lobe with the Pirro Nord and Venta Micena bisons but wider posterior one, whereas it shows similarly wide posterior lobe but narrower anterior one than *B. schoetensacki* from Mauer and Süssenborn, Voigtstedt sample and *B. menneri*, occupying a particular place on the graph (Fig. 14).

A metrical comparison of the metapodials (Fig. 15A, B) clearly distinguishes the Untermassfeld bison from the rest of examined taxa mainly because of the great lengthiness and relative narrowness of both metacarpals and metatarsals irrespective of sex (see also Sher 1997; Maniakas & Kostopoulos 2017a). The metapodials of the bisons from Venta Micena, Sainzelles and Nihowan are proportionally similar each other, slightly wider distally than those of *L. etruscus* (especially the male ones) and as wide as those of the Untermassfeld bison but significantly shorter. Two (D2812 and D2288) of the three complete matacarpals referred by Bukshianidze to *B.* (*E.*) *georgicus* are quite longer and much narrower distally than D3426, features that place them closer to *Leptobos* and *B.* (*E.*) *palaeosinensis*; conversely D3426 groups with metacarpals of Mygdonia bison and it may represent a second taxon in Dmanisi. The Mygdonia and Pirro Nord bisons, are placed proportionally in between Venta Micena/Nihowan and the late Early-Middle Pleistocene bisons from Vallonet, Süssenborn, Mosbach and Mauer. The metapodials of the Mygdonia, Pirro Nord, and Capena group of bisons are as long as those of *L. etruscus* but significantly wider distally. The bison metapodials from Durfort, Vayssiere, and Soleilhac, France (referred to *B. schoetensacki*; Brugal 1995; Brugal & Fosse 2005; Brugal & Lacombat 2005), as well as Kayri, and Salcia, Moldova (Croitor 2010, 2016) are best grouped with the Mygdonia ones, whereas the single known complete metacarpal from Trlica 10-11 (Crégut-Bonnoure & Dimitrijević 2006) appears dimensionally closer to a possible female metacarpal from Pirro Nord. The Norfolk sample of bison metapodials gives conflicting results, with some specimens approaching female *B. priscus* with their shorteness and distal wideness and some others being closer to the Mygdonia/Durfort proportions. The Tiraspol metacarpals (referred to either as *B. schoetensacki* or *B. priscus*; e.g. Croitor 2010 and references therein) are proportionally more similar to the Mygdonia sample but with a distinct tendency for being larger and wider distally.

A PCA analysis of the metapodial shape variation following Scott & Barr (2014) methodology (e.g. Maniakas & Kostopoulos 2017a) (Fig. 16) provides additional results. Metacarpals of the Early Pleistocene European bisons (Fig. 16A) are clearly separated from those of *L. etruscus* along the PC1 axis (accounted for 55.2% of the total variance), which mainly divides long and narrow metacarpals at the negative end from those with shorter lengths and deep distal epiphyses at the positive end. Among bisons, the Venta Micena metacarpals are also distinguished from those from Mygdonia basin along the PC2 axis (accounted for 20.3% of the total variance), which divides longer and deeper proximally metacarpals at the positive end from wider and shallower ones at the negative end. The single available complete Nihowan metacarpal is placed on the positive extreme of this shape variance and close to Venta Micena, whereas the single metacarpal of *B. schoetensacki* from Süssenborn at the negative extreme and at the edges of the Mygdonia morphospace. The single complete metacarpal from Sainzelles lies in the intersection zone between Untermassfeld and Mygdonia, whereas the Pirro Nord/Capena sample well within the Mygdonia shape range. The Untermassfeld taxon seems to occupy an intermediate position in the morphospace between those of Venta Micena and Mygdonia, representing a distinct type of metacarpals, i.e., long with deep proximal and distal epiphyses (e.g. Sher 1997; Maniakas & Kostopoulos 2017a).

Metatarsals from all examined samples show great overlapping along both the PC1 and PC3 axes accounted for 28.5% and 18.0% of the total variance respectively (Fig. 16B). Two main groups are distinguished, however, along the PC2 axis (accounted for 23.7% of the total variance). Long metatarsals, robust at the middle of the diaphysis are placed at the positive end, separated from those having wide distal epiphyses at the negative end. *Leptobos etruscus* and *B. schoetensacki* from Süssenborn occupy these two extremes, respectively. The Nihowan, Venta Micena and Sainzelles metatarsals are also placed toward the positive spectrum of the PC2 axis, well-separated from those from Mygdonia, Pirro Nord/Capena and Untermassfeld that are placed toward the negative end. Untermassfeld and Mygdonia samples show great overlapping along both the PC1 and PC2 axes, with the latter having, however, constantly a narrower diaphysis (MML) than the former. In this respect, the two available metatarsals from Pirro Nord/Capena appear more similar in shape to those from Untermassfeld though significantly shorter (Fig. 16B).

DISCUSSION

Flerov (1972) (*fide* Flerov 1979; Sala 1987; Bukshianidze 2005), proposed erecting the subgenus *Bison* (*Eobison*), uniting Early Pleistocene small bisons with horncores placed rather forward on the cranium and directed latero-caudally. According to the original diagnosis by Flerov (1979), *Eobison* crania are strongly narrowing behind the horncores and characterized by long horncore pedicles, raised forehead, deep and wide temporal fossae, reduced in size and trapezoidal in shape occiput, weakly

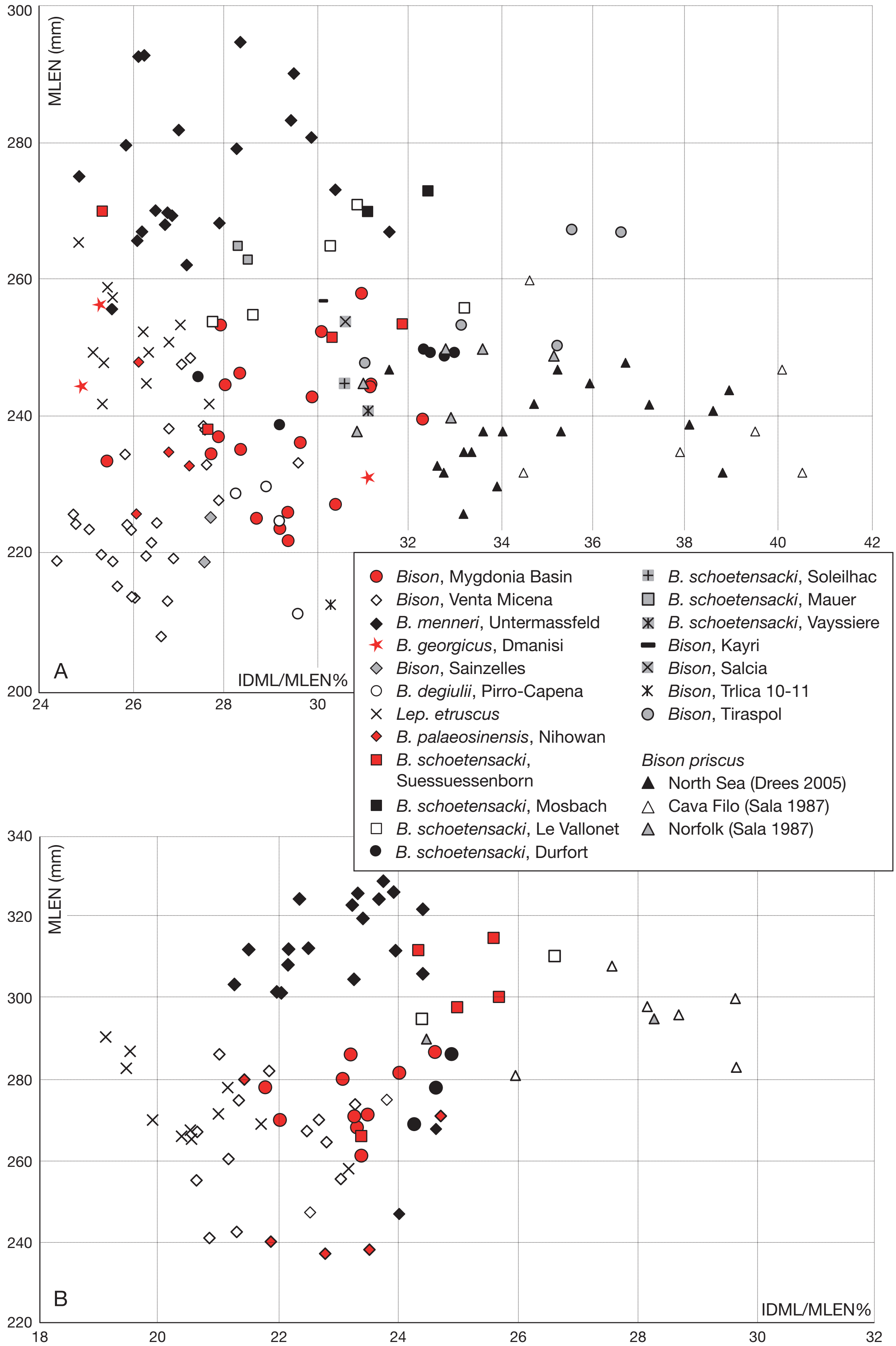

FIG. 15. — Bivariate diagram of the metapodial length (**MLEN**) and robusticity (IDML/MLEN %) comparing *Leptobos etruscus* Falconer, 1859 and several Eurasian *Bison* Hamilton Smith, 1827 samples and species: **A**, metacarpal III+IV; **B**, metatarsal III+IV. Abbreviation: **IDML**, greatest mediolateral diameter of inferior aspect of distal epiphysis.

tubular eye sockets, short frontals elevated between the horns (so as the highest point of the cranium is placed approximately on the level of the lower edge of horncore bases), mandible with short symphysis, straight horizontal, vertical ascending ramus, and an angular process projecting caudally to the level of the condyloid process. Flerov (1972, 1979) included in his *B.* (*Eobison*) three Early Pleistocene Eurasian representatives, i.e., the Chinese *Bison palaeosinensis* indicated as the type species of the subgenus, the Indian *Bison sivalensis* Lydekker, 1878, and *Bison tamanensis* from Azov Sea. Masini (1989) added later *Bison* (*Eobison*) *degiulii* from Italy (see also Masini *et al.* 2013), and Bukshianidze (2005) transferred to the same subgenus *Dmanisibos georgicus* Burchak-Abramovich & Vekua, 1994 from Dmanisi, Georgia.

Although *Eobison*, has long been used as a reference for Early Pleistocene bisons from Eurasia (e.g. Sala 1987; Masini 1989; Kostopoulos 1997; Bukshianidze 2005; Brugal & Lacombat 2005; Masini *et al.* 2013; Croitor 2016; Tong *et al.* 2016) its concept remains questionable. Apart from the type-species *B.* (*E.*) *palaeosinensis*, recently revised by Tong *et al.* (2016), only *B.* (*E.*) *georgicus* meets most of the diagnostic criteria set by Flerov (1979) for the subgenus. Opinions on *B. sivalensis* from Siwaliks diverge substantially among scholars (e.g. Skinner & Kaisen 1946; Flerov 1979: 50, 51; McDonald 1981; Tong *et al.* 2016) and taxonomic decisions would unfortunately be based solely on data provided by Lydekker (1878) as the material ascribed to this taxon appear to be lost (Bukshianidze, pers. com. 2016). Additional material from Siwaliks (Khan *et al.* 2010) is too fragmentary and from inadequate stratigraphic context for safe conclusions.

The taxonomic status of *B.* (*E.*) *tamanensis* is also vague. The taxon was inappropriately designated by Verestchagin (1959) and later validated by Flerov (1979: 52) (for a complete taxonomic history of the species see Croitor 2016), who emphasized the relative position, size, and direction of the pedicles and horncores, and the large temporal fossae together with some occipital characters, which are, however, barely recognized in the severely destroyed holotype (according to published illustrations and photos kindly provided by V. Titov). Kahlke (1999), Croitor & Brugal (2007) and Croitor (2016) indicate *Bison suchovi* Alekseeva, 1967 from Dolinskoye (or Dolinskoe) near Odessa as a junior synonym of *B. tamanensis* but Sher (1997) based on metatarsal proportions from the same site hints that they may represent a more advanced bison taxon. The holotype of *B. suchovi* is a horncore of a rather young and female individual (i.e., Kahlke 1999; Croitor 2016) and thus of limited taxonomic practicability. Baigusheva (2000; see also Croitor 2016) also refers to as *Bison* cf. *tamanensis* a fairly complete cranium from Semibalki in Taman Peninsula but the overall cranial size, the shape, size and advanced dorsoventral compression of the horncores, the strongly tubular orbits, and the lengthened nasals and facial region (according to illustrations provided by V. Titov), might in fact indicate closer affinities to *B. schoetensacki*. According to Croitor (2016: 15) "*the type of* B. (*Eobison*) *tamanensis* […] (comes) [...] *from the post-Villafranchian fauna of Tzimbal*", from where the same author (Croitor 2010, 2016) refers a radius to *B.* cf. *menneri*. Though we cannot exclude the presence of two bisons in the same faunal context, the situation is questionable at least and needs further documentation. Finally, our comparison indicates more derived features for the Taman Peninsula taxon (i.e., the lateral insertions of the horncores and the shortened pedicles) compared to the Dmanisi or Nihowan taxa. Based only on the single and severely incomplete holotype, any decision about the taxonomic status of *B. tamanensis* seems unfounded and it would be better to consider this taxon as a *species inquirenda.* Croitor & Brugal (2007: 259) suggest including the Apollonia bison, known mainly by dental and postcranial remains, into *B. tamanensis.* Nevertheless, a direct assignment of some postcranials from Ukrainian localities to *B. tamanensis* (David & Svistun 1981) has been already challenged by Sher (1997: 174) and there is not in our knowledge other postcranial or dental remains definitely ascribed to the Taman species (e.g. Croitor 2010). Besides, our previous comparison indicates significant differences between the KLT cranium and the holotype of *B. tamanensis.*

The Mygdonia early bison is characterized by small body size (*c.* 600 kg) and cranium, and short and moderately wide metapodials. The female cranium is diagnosed by small horncores of oval basal cross section set closely to the orbits and not widely apart each other, implanted laterally-posterolaterally and on short pedicles that bent weakly down. The frontals are quite long and moderately wide in their supraorbital part. The occipital is trapezoidal shaped and moderately wide with the dorsocaudal margins of the temporal fossae having a lateral position and being quite wide apart each other. The dentition is typically bisontine with moderately short premolars compared to the molars and wide intermediate lobe of m3. The absence of tubular eye sockets, the weakly obtuse coronal angle and the weakly flexed frontals are primitive features shared with other early bisons and differentiating the Mygdonia taxon from the Middle-Late Pleistocene and extant taxa. The Mygdonia early bison differs from *B. menneri, B.* (*E.*) *palaeosinensis*, and *B.* (*E.*) *georgicus* by most morphometrical cranial features, as well as by its more derived metapodial proportions. The contemporaneous bisons from Venta Micena and Sainzelles are dentally similar to the Mygdonia taxon but with narrower p3, p4 and m3, less derived metapodials and shorter metacarpals compared to the metatarsals.

Made *et al.* (2017: figs. 9, 11) indirectly attributes the Apollonia bison to *B. schoetensacki*. As it has been shown, however, cranial, dental and postcranial features of the Mygdonia bison are less derived than those of the late Early to Middle Pleistocene representatives of this species. Among early Mid-Pleistocene bisons referred to as *B. schoetensacki*, the Mygdonia taxon resembles better that from Durfort (France; Brugal 1995), from which, differs in the less short metacarpals compared to metatarsals and the slightly smaller dentition. It seems, however, that the current taxonomic context of *B. schoetensacki* is fuzzy (compare, for example, Le Vallonet vs Durfort metapodial samples) and needs to be revised.

The Mygdonia early bison shares with the Italian *B. degiulii* similarly long and anteriorly narrow frontals, widely apart temporal fossae, and short cranial segment between orbits

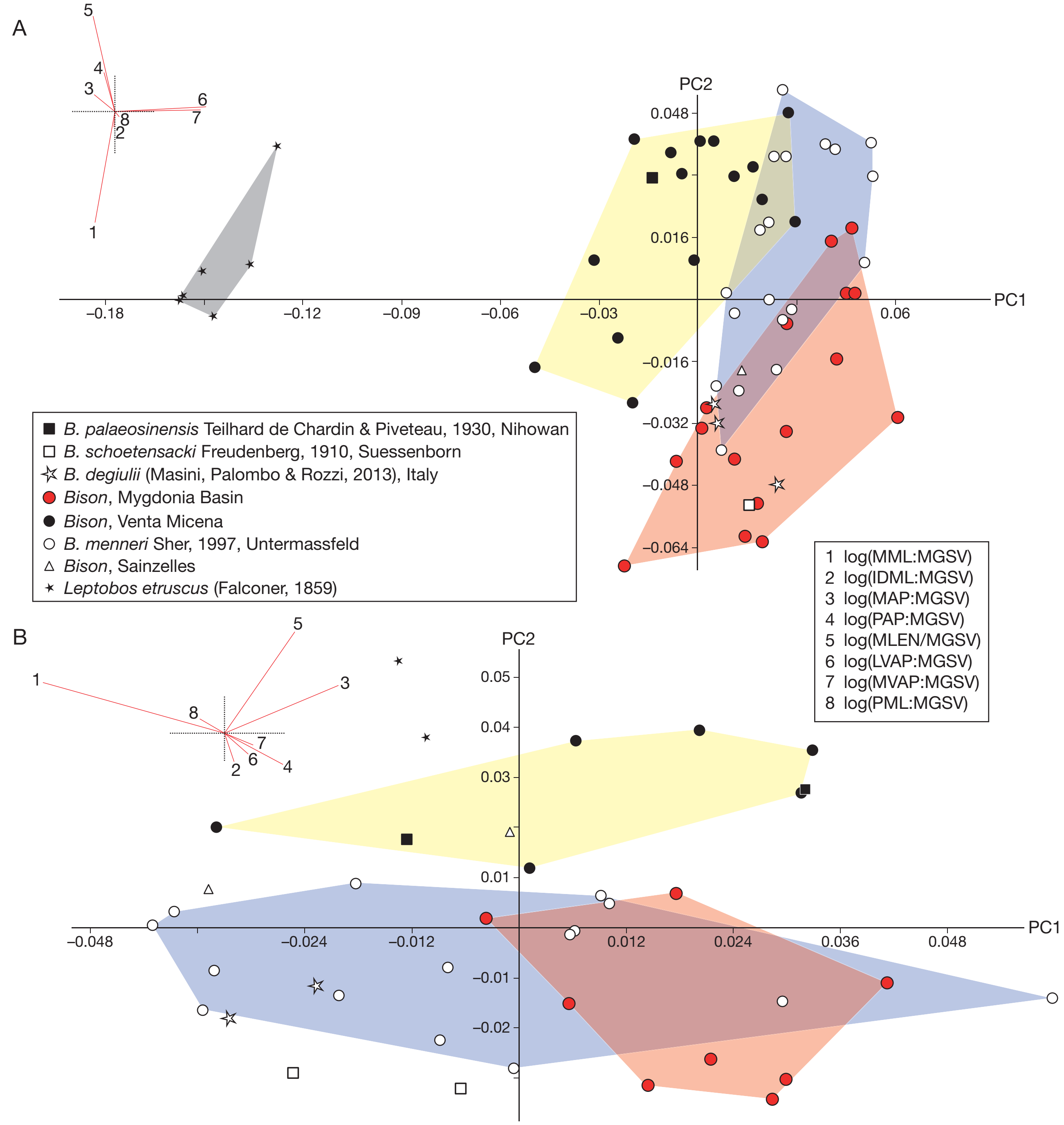

Fig. 16. — Plot of metacarpal III+IV (**A**) and metatarsal III+IV (**B**) scores on principal components (**PC**) 1 and 2 obtained from the Principal Component Analysis (**PCA**) of 8 size-adjusted morphometric variables (following Scott & Barr 2014; see Maniakas & Kostopoulos 2017a). Original raw data. Metapodial measurements: **MLEN**, maximum length; **PAP**, proximal epiphysis anteroposterior diameter; **PML**, proximal epiphysis mediolateral (transverse) diameter; **MAP**, midshaft (determined using MLEN) anteroposterior diameter; **MML**, midshaft mediolateral diameter; **MVAP**, medial trochear verticilli anteroposterior diameter; **LVAP**, lateral trochlear verticilli anteroposterior diameter; **IDML**, inferior aspect of distal epiphysis greatest mediolateral diameter; **MGSV**, Metapodial Global Size Variable (see Scott & Barr 2014).

and horncores. Metapodials of the older Mygdonia population from Tsiotra Vryssi (TSR) are proportionally identical to those from Pirro Nord and Capena, and slightly smaller at the average than those from Apollonia. Cranial metrical differences between KLT and *B. degiulii* are comparable to those between male and female individuals of *B. bonasus* and would be, therefore, attributed to sexual dimorphism. Nevertheless, the Italian taxon displays a significantly smaller dentition, and possibly longer postcornual part of the cranium [the chord bregma to inion is reported as 83.0 mm in the Pirro Nord cranium (Masini 1989) against 47.5 mm in KLT]. Whether these differences merit a taxonomic distinction is hard to prove at the moment, mainly due to the absence of sufficient crania from both areas and statistically conclusive dental and postcranial material especially from the Italian Peninsula. Given the metapodial overlapping between TSR and Pirro Nord and the progressiveness seen in most morphometric features between TSR and APL bison populations we think that all Mygdonia samples would belong to the same taxon, representing a single evolving species. Therefore, we suggest the Mygdonia bison as plausibly conspecific with the Pirro Nord taxon and we refer it to as *Bison* cf. *degiulii*.

Croitor & Brugal (2007) suggested that the Pirro Nord bison might represent an endemic variety of *B. tamanensis* (in their wider concept of this taxon) but we found this assumption rather groundless, especially in the light of new findings from Mygdonia Basin in Greece, Trlica 10-11 in Montenegro (Crégut-Bonnoure & Dimitrijević 2006; Vislobokova & Agadjanian 2015) and some Moldovan sites (Croitor 2010, 2016).

Masini (1989), Sher (1997), Masini *et al.* (2013), and Tong *et al.* (2016) considered the Early Pleistocene bison from Pirro Nord in Italy as member of *B.* (*Eobison*) but Bukshianidze (2005) regarded it as a primitive true bison, *Bison* (*Bison*). We are inclined towards the latter hypothesis, supported by the shortened postcornual part of the cranium, the widely apart and lower positioned caudal parts of the temporal fossae, and the short pedicles that do not rise above the frontal level, features seen in both the Pirro Nord and KLT crania.

A direct descent of the Untermassfeld bison from *Eobison* has been already negated by Sher (1997). Among other European early bisons, the Venta Micena taxon and the most likely conspecific Sainzelles population show postcranial proportions similar to those of *B.* (*E.*) *palaeosinensis* but with an already much more derived shortening of the metacarpals compared to the metatarsals. Venta Micena may in fact represent the only current record of *B.* (*Eobison*) in Europe but the single preserved partial cranium from this site (VM 8000) appears more advanced than the Dmanisi or Nihowan taxa and rather closer to a true bison condition, especially if it is taken into account that it likely represents a young female in which cranial features would appear more plesiomorphic.

Other Asian specimens (e.g. the partial cranium No 11.313 from Loc. 42 SE Shansi/Yushe III in Teilhard de Chardin & Trassaert 1938 and Tong *et al.* 2016; the horncores PUPC 5/13 and PUPC 5/14 in Khan *et al.* 2010) and taxa (i.e., *Adjiderebos cantabilis* Dubrovo & Burchak-Abramovich, 1986; *Protobison kushkunensis* Burchak-Abramovich, Gadzhiev & Vekua, 1980; *Probison dehmi* Shani & Khan, 1968) are, of more questionable affinities and though some of them may be crucial for the re-evaluation *B.* (*Eobison*) concept, the available data have to be revised in the light of present day knowledge. They demonstrate, however, the significant radiation underwent by the Asian Bovini during the Early Pleistocene in accordance with nuDNA data (Xie *et al.* 2010; Hassanin *et al.* 2013).

Bison first occurrence in the Greek fossil archive is definitely recorded in the uppermost levels of the Gerakarou Formation of Mygdonia Basin, in the fossil site of Tsiotra Vryssi that marks the first part of the post-Olduvai Pleistocene. Bisons are absent from the slightly older fauna of Gerakarou, where *E. altidens* makes its first local appearance (Gkeme *et al.* 2017) joining typically Villafranchian faunal elements such as *Eucladoceros*, *Croizetoceros* and *Gazella*. In the Tsiotra Vryssi fauna early bison associates among others *Leptobos, Pontoceros, Palaeotragus, Metacervocerus rhenanus, Pacycrocuta brevirostris*, *Ursus etruscus*, and *Canis etruscus* (Konidaris *et al.* 2015 and pers. data). A comparable mammal association is recorded outside Mygdonia Basin, in Libakos (Western Macedonia) where, however, *Dama vallonetensis* 'replaces' *M. rhenanus* and hippopotamus occurs. Though bison is not recorded in the Libakos fauna, one lower m3 from the neighboring but much poorly known fauna of Polylakkos referred to as *Leptobos*? by Steensma (1988) may in fact represent a *Bison*. As in Gerakarou and Libakos, the Polylakkos faunal assemblage includes *Equus altidens* (Gkeme *et al.* 2017). Leptobovine bovids still associate bisons in the slightly younger and hippopotamus bearing fauna of Kalamoto-2 and the roughly isochronous Krimni, from which however giraffids are missing and large to giant deer increase their signal. Bisons became soon after the only and dominant large bovid and one of the prevalent herbivores of the Greek mammal communities, as displayed in the slightly younger fauna of Apollonia-1, where bisons associate new carnivore elements such as *Lycaon* ex. gr. *lycaonides*, *Canis* ex gr. *mosbachensis* and a small *Megantereon*, as well as a variety of caprines/ovibovines. The later local history of bisons is less known, hidden by the absence of adequate mid-Pleistocene sampling. Bisons appear in the late Middle Pleistocene faunas of Petralona cave (N. Greece) (Tsoukala 1989) and in Megalopolis Basin (S. Greece; Melentis 1966) with heavy priscoid forms that at the same time were rapidly expanding in the rest of Europe together with primitive oxen.

The first local record of bisons seems to coincide with that in Trlica 10-11, Montenegro dated at the lower part of the post-Olduvai – pre-Jaramillo Pleistocene (Vislobokova & Agadjanian 2015). As in Tsiotra Vryssi, *Bison* and *Leptobos* co-exist in Trlica 10-11. Although no co-occurrence of the two genera has been so far reported into the same faunal context from Italy (Masini *et al.* 2013), the earliest local bison record from Mugello is placed in Farnetta Faunal Unit (FU), otherwise yielding *Leptobos* (e.g. in Pietrafitta). These data rather suggest that *Bison degiulii* dispersal event in the Balkano-Italian territory was rather simultaneous. In Italy, *B. degiulii* is well known from Pirro FU, in a faunal context roughly equivalent to that from Apollonia-1, whereas recent data from Ellera di Corciano (Cherin *et al.* 2012) and Cava Redicicoli (Marra *et al.* 2014) extend its presence up to *c.* 0.8 Ma.

CONCLUSIONS

Bisons originally invaded Southern Balkans between 1.7-1.5 My with a small primitive form similar to the contemporaneous *B. degiulii* from Italy. The taxon most likely represents one of the first representatives of true bison, *Bison* (*Bison*). At the same time in Western Europe another primitive bison appear in Venta Micena, Spain but its relations to either *B.* (*Bison*) or *B.* (*Eobison*) remain unclear. Governed by global climatic and regional environmental changes, the arrival of bisons in Southern Balkans also marks the last local occurences of leptobovine bovids, though a direct relation between these two events is not as obvious as supposed at first sight. In fact early *Bison* and *Leptobos* appear to shortly co-exist in the faunal assemblages of this period, as documented by the Greek and Montenegro fossil record at least. *Leptobos* fade possibly out before Cobb Mt. subchron, leaving *Bison* as the predominant large bovid of local mammal communities. An appendicular palaeodemographic analysis of the Apollonia population of this period (Appendix 4) indicates strong social resemblances to the extant American bison and European wisent, though the Greek species is of different ecological profile (i.e., Maniakas & Kostopoulos 2017a, b). During the post-Olduvai-pre-Jaramillo time span the Mygdonia bison underwent a series of changes, such as a weak increase in size, a strengthening of the dentition by cement and a widening of metapodials associated by an increase of the distal trochlear splaying, altogether representing adaptations to progressively harsher environmental conditions (see discussion in Maniakas & Kostopoulos 2017a, b).

The comparison among early bison populations across Europe, as well as with Mid-Pleistocene representatives indicates a much more complex evolutionary and biogeographic history than previously thought, an issue that needs to be further addressed.

Acknowledgements

We are particularly grateful to Hao-Wen Tong (Key Laboratory of Vertebrate Evolution and Human Origins of Chinese Academy of Sciences), Vadim Titov (Institute of Arid Zones SSC RAS, Russian Academy of Science), George Konidaris (Eberhard Karls University of Tübingen, Senckenberg Center for Human Evolution and Palaeoenvironment), Maia Bukhsianidze (Georgian National Museum), Pierre-Elie Moullé (Musée de Préhistoire Régionale de Menton, France), Evelyn Crégut-Bonnoure (Muséum Requien, Avignon), Jean-Philippe Brugal (CNRS, France), Marzia Breda (Natural History Museum, London), and Jan van der Made (National Museum of Natural History, Madrid) for sharing raw data, articles, photographic material and expertise. The excavations in the locality Tsiotra Vryssi were supported from 2014 to 2016 by the ERC STG no. 283503 PaGE ('Paleoanthropology at the Gates of Europe: Human evolution in the southern Balkans') and in 2017 by the ERC COG no. 724703 CROSSROADS ('Human Evolution at the Crossroads'), both leaded by Prof. K. Harvati (Eberhard Karls University of Tübingen, Senckenberg Center for Human Evolution and Palaeoenvironment). J.Ph. Brugal and H.-W. Tong are deeply thanked for their fruitful comments and suggestions that help us improve this manuscript.

REFERENCES

Bärmann E. V. & Rössner G. 2011. — Dental nomenclature in Ruminantia: Towards a standard terminological framework. *Mammalian Biology* 76: 762-768. https://doi.org/10.1016/j.mambio.2011.07.002

Baigusheva V. S. 2000. — New data on Tasmanian faunal assemblage from the excavation site near Semibalki village (Azov Area). *Historical-Archaeological in Azov and Lower Don in 1998* 16: 27-57 (in Russian).

Brugal J.-Ph. 1985. — Les *Bos primigenius* Boj., 1827 du Pléistocène moyen des Grottes de Lunel-Viel (Herault). *Bulletin du Musée d'Anthropologie préhistorique de Monaco* 28: 7-62.

Brugal J.-Ph. 1995. — Le bison (Bovidae, Artiodactyla) du Pléistocène moyen ancien de Durfort (Gard, France). *Bulletin du Muséum national d'histoire naturelle, 4ème série, section C, Sciences de la terre, paléontologie, géologie, minéralogie* 16 (2-4): 349-381. https://biodiversitylibrary.org/page/55848401

Brugal J.-Ph. & Fosse Ph. 2005. — Les grands bovidés (*Bison* cf. *schoetensacki*) du site Pleistocène moyen de la Vayssière (Aveyron, France), *in* Cregut-Bonnoure E. (ed.), Les ongulés holarctiques du Pliocène et du Pléistocène. *Quaternaire* h.s. 2: 75-80.

Brugal J.-Ph. & Lacombat F. 2005. — *Bison schoetensacki* (Freudenberg, 1910), *in* Lacombat F. (ed.), Les grands Mammifères fossiles du Velay – Les collections paléontologiques du Plio-Pléistocène du Muzée Crozatier, le Puy-en-Velay. *Annales des Amis du Musée Crozatier* 13-14: 113-115.

Bukshianidze M. 2005. — *The Fossil Bovidae of Dmanisi*. PhD dissertation, University of Ferrara, Italy, 192 p. (unpublished).

Caughley G. 1965. — Mortality patterns in mammals. *Ecology* 47 (6): 906-918. https://doi.org/10.2307/1935638

Cherin M., Bizzarri R., Buratti N., Caponi T., Grossi F., Kotsakis T., Pandolfi L., Pazzaglia F. & Barchi M. R. 2012. — Multidisciplinary study of a new Quaternary mammal-bearing site from Ellera di Corciano (central Umbria, Italy): preliminary data. *Rendiconti Online della Società Geologica Italiana* 21: 1075-1077.

Cherin M., D'Allestro V. & Masini F. 2017. — New bovid remains from the Early Pleistocene of Umbria (Italy) and a reappraisal of *Leptobos merlai*. *Journal of Mammalian Evolution* (in press; published online; https://doi.org/10.1007/s10914-017-9421-x).

Crégut-Bonnoure E. & Dimitrijević V. 2006. — *Megalovis balcanicus* sp. nov. and *Soergelia intermedia* sp. nov. (Mammalia, Bovidae, Caprinae), new Ovibovini from the Early Pleistocene of Europe. *Revue de Paléobiologie* 25: 723-773.

Croitor R. & Brugal J.-Ph. 2007. — New insights concerning Early Pleistocene cervids and bovids in Europe. *Courier Forschungsinstitut Senckenberg* 259: 47-59.

Croitor R. 2010. — Critical remarks on genus *Bison* (Bovidae, Mammalia) from Pleistocene of Moldova. *Revista Arheologocă* s.n. 5: 172-188 (in Russian).

Croitor R. 2016. — Genus *Bison* (Bovidae, Mammalia) in Early Pleistocene of Moldova. *Materialele Conferinței științifice naționale cu participare internațională "Mediul și dezvoltare durabilă"*, Ediția a III-a, Chișinău: 14-20. https://hal.archives-ouvertes.fr/hal-01766112

David A. & Svistun V. I. 1981. — *Bison* remains from Upper Pliocene and Lower Pleistocene deposits of Moldova and South Ukraine, *in Biostratigraphy of Anthropogene and Neogene of South-West of USSR*. Ştiinţa, Chişinău: 3-15 (in Russian).

Discamps E. & Costamagno S. 2015. — Improving mortality profile analysis in zooarchaeology: a revised zoning for ternary diagrams. *Journal of Archaeological Science* 58: 62-76. https://doi.org/10.1016/j.jas.2015.03.021

Drees M. 2005. — Sexual dimorphism in Pleistocene *Bison priscus* (Mammalia, Bovidae) with a discussion on the position of *Bison schoetensacki*. *Senckenbergiana Lethaea* 85 (1): 153-157. https://doi.org/10.1007/BF03043424

Empel W. 1962. — Morphologie des Schädels von *Bison bonasus* (Linnaeus, 1758). Bisoniana VI. *Acta Theriologica* 6: 53-111.

https://doi.org/10.4098/AT.arch.62-4

Erickson G. M., Currie P. I., Inouye B. D. & Winn A. A. 2010. — A revised life table and survivorship curve for Albertosaurus sarcophagus based on the Dry Island mass death assemblage. *Canadian Journal of Earth Sciences* 47: 1269-1275. https://doi.org/10.1139/E10-051

Fischer K.-H. 1965. — Bison reste (*Bison schoetensacki voigtstedtensis* ssp. n.) aus den altpleistozänen Tonen von Voigtstedt in Thüringen. *Palaeontologische Abh A III* (2/3): 489-520.

Flerov C. C. 1972. — *Dryevnyeyshiye pryedstavityelya i istoriya roda Bison* [The most ancient bisons and the history of genus *Bison*]. Teriologia 1, Nauka, Novosibirsk (in Russian).

Flerov C. C. 1979. — Sistematika i evolûziâ [Systematics and evolution], *in* Sokolov V. E. (ed.), *European Bison: Morphology, Systematics, Evolution, Ecology*. Nauka, Moscow: 9-127 (in Russian).

Gee H. 1993. — The distinction between postcranial bones of *Bos primigenius* Bojanus, 1827 and *Bison priscus* Bojanus, 1827 from the British Pleistocene and the taxonomic status of *Bos* and *Bison*. *Journal of Quaternary Science* 8: 79-92. https://doi.org/10.1002/jqs.3390080107

Geraads D. 1992. — Phylogenetic analysis of the tribe Bovini (Mammalia, Artiodactyla). *Zoological Journal of the Linnean Society* 104: 193-207. https://doi.org/10.1111/j.1096-3642.1992.tb00922.x

Gkeme A., Koufos G. D. & Kostopoulos D. S. 2017. — The Early Pleistocene stenonoid horse from Libakos and Polylakkos (Western Macedonia, Greece): biochronological and palaeoecological implications and dispersal events. *15th Congress of the Regional Committee on Mediterranean Neogene Stratigraphy*, Book of Abstracts, Athens: 67.

Gromova V. 1935. — [Die vorweltliche Wisent (*Bison priscus* Bojanus) in USSR]. *Travaux de l'Institut paléozoologique de l'Académie des Sciences de l'URSS* 2: 77-204 (in Russian with German summary).

Groves C. 1981. — Systematic relationships in the Bovini (Artiodactyla, Mammalia). *Zietschrift für Systematische Zoologie und Evolutions forschung* 19: 264-278. https://doi.org/10.1111/j.1439-0469.1981.tb00243.x

Groves C. & Grubb P. 2011. — *Ungulate Taxonomy*. The John Hopkins University Press, Baltimore, 309 p.

Hammer Ø., Harper D. A. T. & Ryan P. D. 2001. — PAST: Paleontological statistics software package for education and data analysis. *Palaeontologia Electronica* 4 (1): 9 p. http://palaeo-electronica.org/2001_1/past/issue1_01.htm

Hassanin A. 2014. — Systematic and Evolution of Bovini, *in* Melletti M. & Burton J. (eds), *Ecology, Evolution and Behavior of Wild Cattle: Implications for Conservation*. Cambridge University Press, Cambridge: 7-20. https://doi.org/10.1017/CBO9781139568098.003

Hassanin A. J., Ropiquet A., Nguyen T. T. & Couloux A. 2013. — Combining multiple autosomal introns for studying shallow phylogeny and taxonomy of Laurasiatherian mammals: Application to the tribe Bovini (Cetartiodactyla, Bovidae). *Molecular Phylogenetics and Evolution* 66: 766-775. https://doi.org/10.1016/j.ympev.2012.11.003.

Hodgson B. H. 1837. — On the *Bibos*, Gauri Gau or Gauríká Gau of the Indian forests. *Journal of the Asian Society* 69: 745-750.

International Commission on Zoological Nomenclature 1999. — *International Code of Zoological Nomenclature. Fourth Edition*. The International Trust for Zoological Nomenclature, London, 306 p.

Kahlke R.-D. 1999. — *The History of the Origin, Evolution and Dispersal of the Late Pleistocene Mammuthus-Coelodonta Faunal Complex in Eurasia (Large Mammals)*. Fenske Companies, Rapid City, 219 p.

Khan M. A., Kostopoulos D. S., Akhtar M. & Nazir M. 2010. — *Bison* remains from the Upper Siwaliks of Pakistan. *Neues Jahrbuch für Geologie und Paläontologie* 258: 121-128. https://doi.org/10.1127/0077-7749/2010/0090

Klein R. G. 1982. — Patterns of Ungulate mortality and Ungulate mortality profiles from Langebaanweg (Early Pliocene) and Elandfontein (middle Pleistocene) South-Western Cape Province, South Africa. *Annals of the South African Museum* 90 (2): 49-94. https://biodiversitylibrary.org/page/40763687

Kobryńczuk F., Krasińska M. & Szara T. 2008. — Sexual dimorphism in skulls of the lowland European bison, *Bison bonasus bonasus*. *Annales Zoologici Fennici* 45: 335-340. https://doi.org/10.5735/086.045.0415

Konidaris G. E., Tourloukis V., Kostopoulos D. S, Thompson N., Giusti D., Michailidis D., Koufos G. D. & Harvati K. 2015. — Two new vertebrate localities from the Early Pleistocene of Mygdonia Basin (Macedonia, Greece): Preliminary results. *Comptes Rendus Palevol* 14: 353-362. https://doi.org/10.1016/j.crpv.2015.05.004

Kostopoulos D. S. 1996. — *The Plio-Pleistocene Artiodactyls of Macedonia (Greece)*. PhD dissertation, Aristotle University of Thessaloniki, 612 p. (in Greek with English summary; unpublished).

Kostopoulos D. S. 1997. — The Plio-Pleistocene artiodactyls of Macedonia 1. The fossiliferous site Apollonia-1, Mygdonia Basin of Greece. *Geodiversitas* 19: 845-875.

Koufos G. D. 2018. — New material and revison of the Carnivora, Mammalia from the Lower Pleistocene locality Apollonia 1, Greece. *Quaternary* 1, 6. https://doi.org/10.3390/quat1010006

Koufos G. D. & Kostopoulos D. S. 1997. — New carnivore material from the Plio-Pleistocene of Macedonia (Greece) with the description of a new canid. *Münchner Geowissenschaftliche Abhandlungen Reihe* A 34: 33-63.

Koufos G. D., Syrides G. E., Kostopoulos D. S. & Koliadimou K. K. 1995. — Preliminary results about the stratigraphy and the palaeoenvironment of Mygdonia Basin, Macedonia, Greece. *Geobios* 28 (suppl. 1): 243-249. https://doi.org/10.1016/S0016-6995(95)80171-5

Krasińska M. & Krasiński Sb. A. 2002. — Body mass and measurement of the European bison during postnatal development. *Acta Theriologica* 47 (1): 85-106. https://doi.org/10.1007/BF03193569

Kurtén B. 1953. — On the variation and population dynamics of fossil and recent mammal populations. *Acta Zoologica Fennica* 76: 1-122.

Legendre S. 1986. — Analysis of mammalian communities from the late Eocene and Oligocene of Southern France. *Palaeovertebrata* 16: 191-212.

Lewis P. J., Buchanan B. & Johnson E. 2005. — Sexing bison metapodials using Principal Component Analysis. *Plains Anthropologist* 50 (194): 159-172. https://doi.org/10.1179/pan.2005.017

Lewis P. J., Buchanan B., Johnson E. & Bement L. 2006. — Sexing Cooper bison metapodials: a test of the PCA method. *Current Research in the Pleistocene* 23: 191-192.

Lydekker R. 1878. — Crania of ruminants from the Indian Tertiaires. *Paleontologia Indica* 10 (1): 88-171.

MacEarchern S., McEwan J. & Goddard M. 2009. — Phylogenetic reconstruction and the identification of ancient polymorphism in the Bovini tribe (Bovidae, Bovinae). *BMC Genomics* 10: 177. https://doi.org/10.1186/1471-2164-10-177

Made J. van der 1999. — Ungulates from Atapuerca TD6. *Journal of Human Evolution* 37: 389-413. https://doi.org/10.1006/jhev.1998.0264

Made J. van der, Rossel J. & Blasco R. 2017. — Faunas from Atapuerca at the Early-Middle Pleistocene limit: The ungulates from level TD8 in the context of climatic change. *Quaternary International* 433: 296-346. https://doi.org/10.1016/j.quaint.2015.09.009

Maniakas I. & Kostopoulos D. S. 2017a. — Morphometric-palaeoecological dis-crimination between *Bison* populations of the western Palaearctic. *Geobios* 50: 155-171. http://dx.doi.org/10.1016/j.geobios.2017.01.001

Maniakas I. & Kostopoulos D. S. 2017b. — Assessing astragalar morphology and biomechanics in western Palaearctic *Bison* populations with geometric morphometrics. *Comptes Rendus Palevol* 16: 783-794. http://dx.doi.org/10.1016/j.crpv.2017.06.003

Marra F., Pandolfi L., Petronioc C., Di Stefano G., Gaeta M. & Salari L. 2014. — Reassessing the sedimentary deposits and vertebrate assemblages from Ponte Galeria area (Rome, central Italy): An archive for the Middle Pleistocene faunas of Europe. *Earth-Science Reviews* 139: 104-122. https://doi.org/10.1016/j.earscirev.2014.08.014

Martínez-Navarro B., Ros-Montoya S., Espigares M. P. & Palmqvist P. 2011. — Presence of the Asian origin Bovini, *Hemibos* sp. aff. *Hemibos gracilis* and *Bison* sp., at the Early Pleistocene site of Venta Micena (Orce, Spain). *Quaternary International* 243: 54-60. https://doi.org/10.1016/j.quaint.2011.05.016

Masini F. 1989. — *I bovini villafranchiani dell'Italia*. PhD dissertation, University of Modena and Florence, Florence, 152 p. (in Italian, unpublished).

Masini F., Palombo M.-R. & Rozzi R. 2013. — A reappraisal of the Early to Middle Pleistocene Italian Bovidae. *Quaternary International* 288: 45-62. https://doi.org/10.1016/j.quaint.2012.03.026

Massilani D., Guimaraes S., Brugal J. P., Bennett E. A., Tokarska M., Arbogast R. M., Baryshnikov G., Boeskorov G., Castel J. C., Davydov S., Madelaine S., Putelat O., Spasskaya N. N., Uerpman H. P., Grange T. & Geigl E. M. 2016. — Past climate changes, population dynamics and the origin of bison in Europe. *BMC Biology* 14 (1): 93. https://doi.org/10.1186/s12915-016-0317-7

McDonald J. N. 1981. — *North American Bison: their Classification and Evolution*. University of California Press, Berkeley, 316 p.

McHugh T. 1958. — Social behavior of the American buffalo (*Bison bison bison*). *Zoologica* 43: 1-40. https://biodiversitylibrary.org/page/51124024

Melentis J. K. 1966. — Studien über fossile Vertebraten Griechenlands. 7. Die Boviden des Jungpleistozäns des Beckens von Megalopolis im Peloponnes (Griechenland). *Annales géologiques des Pays helléniques* 16: 446-472.

Moyà-Solà S. 1987. — Los bóvidos (Artiodactyla, Mammalia) del yacimiento del Pleistoceno inferior de Venta Micena (Orce, Granada, España). *Paleontologia i Evolució*, memoria especial 1: 181-236.

Olsen S. J. 1960. — Postcranial skeletal characters of *Bison* and *Bos*. *Papers of the Peabody Museum of Archaeology and Ethnology, Harvard University* 35 (4): 1-15. https://doi.org/10.2307/278755

Pilgrim G. E.1939. — The fossil Bovidae of India. *Memoirs of the Geological Survey of India, Palaeontologia Indica*, n.s. 26 (1), 356 p.

Plumb G. E., White P. J. & Aure K. 2014. — American bison *Bison bison* (Linnaeus, 1758), *in* Melletti M. & Burton J. (eds), *Ecology, Evolution and Behavior of Wild Cattle: Implications for Conservation*. Cambridge University Press, Cambridge: 83-114. https://doi.org/10.1017/CBO9781139568098.011

Reinhardt V. 1985. — Social behavior in a confined bison herd. *Behaviour* 92: 209-226.

Sala B. 1987. — *Bison schoetensacki* Freud. from Isernia la Pineta (Early Mid-Pleistocene – Italy) and revision of the European species of bison. *Paleontographia Italica* 74: 113-170.

Schertz E. 1936. — Zur Unterscheidung von *Bison priscus* Boj. und *Bos primigenius* Boj. an Metapodien und Astragalus, nebst Bemerkungen über einige diluviale Fundstellen. *Seckenbergiana* 18: 37-71.

Scott E. 2010. — Extinctions, scenarios, and assumptions: Changes in latest Pleistocene large herbivore abundance and distribution in western North America. *Quaternary International* 217: 225-239. https://doi.org/10.1016/j.quaint.2009.11.003

Scott K. M. 1983. — Prediction of body weight of fossil Artiodactyla. *Zoological Journal of the Linnean Society* 77: 199-215. https://doi.org/10.1111/j.1096-3642.1983.tb00098.x

Scott R. S. 2004. — *The Comparative Paleoecology of Late Miocene Eurasian Hominoids*. PhD dissertation, the University of Texas at Austin, 458 p. (unpublished).

Scott R. S. & Barr W. A. 2014. — Ecomorphology and phylogenetic risk: Implications for habitat reconstruction using fossil bovids. *Journal of Human Evolution* 73: 47-57. https://doi.org/10.1016/j.jhevol.2014.02.023

Sher A. V. 1997. — An Early Quaternary bison population from Untermaßfeld: *Bison menneri sp.* nov., *in* Kahlke R.-D. (ed.), Das Pleistozän von Untermaßfeld bei Meiningen (Thüringen), Teil 2. *Monographien des Römisch-Germanischen Zentralmuseums Mainz* 40: 101-180.

Skinner M. R. & Kaisen O. C. 1946. — The fossil *Bison* of Alaska and preliminary revision of the genus. *Bulletin of the American Museum of the Natural History* 89: 123-256. http://hdl.handle.net/2246/399

Soubrier J., Gower G., Chen K., Richards S. M., Llamas B., Mitchell K. J., Ho S. Y. W., Kosintsev P., Lee M. S. Y., Baryshnikov G., Bollongino R., Bover P., Burger J., Chivall D., Cregut-Bonnoure E., Decker J. E., Doronichev V. B., Douka K., Fordham D. A., Fontana F., Fritz C., Glimmerveen J., Golovanova L. V., Groves C., Guerreschi A., Haak W., Higham T., Hofman-Kaminska E., Immel A., Julien M. A., Krause J., Krotova O., Langbein F., Larson G., Rohrlach A., Scheu A., Schnabel R. D., Taylor J. F., Tokarska M., Tosello G., van der Plicht J., van Loenen A., Vigne J. D., Wooley O., Orlando L., Kowalczyk R., Shapiro B. & Cooper A. 2016. — Early cave art and ancient DNA record the origin of European bison. *Nature Communications* 7: 13158. https://doi.org/10.1038/ncomms13158

Steele T. E. 2003. — Using mortality profiles to infer behavior in the fossil record. *Journal of Mammalogy* 84 (2): 418-430. https://doi.org/10.1644/1545-1542(2003)084<0418:UMPTIB>2.0.CO;2

Steensma K. J. 1988. — *Plio-/Pleistozäne Großsäugetiere (Mammalia) aus dem Becken von Kastoria/Grevena, südlich von Neapolis-NW-Griechenland*. PhD dissertation, Technical University of Clausthal, 315 p. (unpublished).

Stiner M. C. 1990. — The use of mortality patterns in archaeological studies of hominid predatory adaptations. *Journal of Anthropological Archaeology* 9 (4): 305-351. https://doi.org/10.1016/0278-4165(90)90010-B

Teilhard de Chardin P. & Piveteau J. 1930. — Les Mammifères fossiles de Nihowan (Chine). *Annales de Paléontologie* 19: 1-154.

Teilhard de Chardin P. & Trassaert M. 1938. — Cavicornia of south-eastern Shansi. *Paleontologia Sinica* n. ser. C, 6: 1-106.

Tong H. W., Chen X. & Zhang B. 2016. — New fossils of *Bison palaeosinensis* (Artiodactyla, Mammalia) from the steppe mammoth site of Early Pleistocene in Nihewan Basin, China. *Quaternary International* 445: 250-268. https://doi.org/10.1016/j.quaint.2016.07.033

Tsoukala E. 1989. — *Contribution to the Study of the Pleistocene Fauna of Large Mammals (Carnivora, Perissodactyla, Artiodactyla) from Petralona Cave, Chalkidiki (N. Greece)*. PhD dissertation, Aristotle University of Thessaloniki, 360 p. (in Greek with English summary; unpublished).

Tsoukala E. & Chatzopoulou K. 2005. — A new Early Pleistocene (Latest Villafranchian) site with mammals in Kalamotó (Mygdonia Basin, Macedonia, Greece) – preliminary report. *Mitteilungen der Kommission für Quartärforschung Österreichische Akademie der Wissenschaften* 14: 213-233.

Vasiliev S. K. 2008. — Late Pleistocene bison (*Bison p. priscus* Bojanus, 1827) from the Southeastern part of Western Siberia. *Archaeology Ethnology & Anthropology of Eurasia* 34 (2): 34-56. https://doi.org/10.1016/j.aeae.2008.07.004

Verestchagin N. K. 1959. — *The Mammals of the Caucasus; a History of the Evolution of the Fauna*. Academia NAUK, Leningrad, 704 p. (translated from Russian; Israel Program for Scientific Translations, Jerusalem 1967). https://doi.org/10.5962/bhl.title.46326

Verkaar E. L., Nijman I. J., Beeke M., Hanekamp E. & Lenstra J. A. 2004. — Maternal and paternal lineages in cross-breeding bovine species. Has wisent a hybrid origin? *Molecular Biology and Evolution* 21: 1165-1170. https://doi.org/10.1093/molbev/msh064

Vislobokova I. & Agadjanian A. K. 2015. — New data on large mammals of the Pleistocene Trlica fauna, Montenegro, the Central Balkans. *Paleontological Journal* 49: 651-667. https://doi.org/0.1134/S0031030115060143

WEGRZYN M. & SERWATKA S. 1984. — Tooth eruption in the European bison. *Acta Theriologica* 29: 111-121. https://doi.org/10.4098/AT.arch.84-9

XIE Y., LI Y., ZHAO X., ZHANG X., LI N., XIE Z., LIU H. & LI Q. 2010. — Origins of the Chinese yak: evidence from maternal and paternal inheritance. *Proceedings of the 4th International Conference on Bioinformatics and Biomedical Engineering*, 5 p. https://doi.org/10.1109/ICBBE.2010.5516521

ZEYLAND J., WOLKO L., LIPIŃSKI Ł., WOŹNIAK A., NOWAK A., SZALATA M., BOCIANOWSKI J. & SŁOMSKI R. 2012. — Tracking of wisent–bison–yak mitochondrial evolution. *Journal of Applied Genetics* 53: 317-322. https://doi.org/10.1007/s13353-012-0090-4

Submitted on 14 November 2017;
accepted on 12 February 2018;
published on 5 July 2018.

APPENDICES

Appendix 1. — Sexing criteria of early *Bison* Hamilton Smith, 1827 crania. Data from Skinner & Kaisen (1946), Empel (1962), McDonald (1981) and personal data. Abbreviations: **Sm-Sm**, maximum width of the cranium at the maxilla; **Ect-Ect**, minimum cranial width at the postorbital constrictions.

	most commonly in:	
Character	**Males**	**Females**
1. Dorsal expression of cornual process	clear-strong	weak-absent
2. Outline of basal horncore cross section	dorsoventrally compressed -broadly triangular (isosceles)	circular to elliptical
3. Relative size of horncore base	large-massive (DAP base ≥ DAP orbit)	slender (DAP base < DAP orbit)
4. Shape of postorbital constriction	concave narrow	concave wide
5. Length of frontals compared to the postorbital width	short	long
6. Shape of the glenoid cavity	flattened transversally (independent from age)	convex (both transversally and caudorostrally; independent form age)
7. Relative development of the mastoids (occipital view)	mastoids strongly expanded laterally and completely surrounding the base of the jugular process (independent from age)	mastoids weakly extended laterally marginally surrounding the base of the jugular process (independent from age)
8. Maxillary volume and Ect-Ect/Sm-Sm index	voluminous maxilla-high index	less voluminous maxilla-lower index
9. Relative width of the nasal bones	wide	narrow
10. Development of the anterior tuberosities of the basioccipital	strong	weaker

Appendix 2. — Crania of early *Bison*. Symbol: *****, Possible sex identification based on criteria set on Appendix 1.

Taxon	**Specimen**	**Sex***	**Basic References**
B. palaeosinensis	Crâne A, Nihowan, China	♂	Teilhard de Chardin & Piveteau 1930; Flerov 1979; Masini 1989; Tong *et al.* 2016
	Crâne B, Nihowan, China	? ♀	
“*B. sivalensis*”	B 239, Tartot-Siwaliks, India	? ♀	Lydekker 1878; Pilgrim 1939; McDonald 1981
B. tamanensis	ZIN 26010/1, Taman peninsula, Russia	? ♂	Verethchagin 1959; Flerov 1979
“*B. cf. tamanensis*”	КП-26386/1, ОП-805 Semibalki, Azov Sea	♂	Baigusheva 2000; Croitor 2016
B. degiulii	IGPB (Universitá di Bari, Italy) no catalogue number, Cava Pirro, Italy	♂	Masini 1989; Masin *et al.* 2013
B. georgicus	D354, Dmanisi, Georgia	♂	Bukshianidze 2005
B. menneri	IQW 1980/17380, Untermassfeld, Germany	♂ young	Sher 1997
Bison sp.	VM8000, Venta Micena, Spain	*c.* ♀ young	Martínez-Navarro *et al.* 2011
B. voigtstedtensis	IQW 1966 / 7 177 (Voi. 26 882),Voigtstedt, Germany	♂	Fischer 1965

APPENDIX 3. — Dental and metapodial measurements of the Mygdonia early bison: **A**, upper toothrows and teeth; **B**, lower toothrows and teeth. Measuremens **in red** represent best estimations.

Appendix 3A	LP2-M3	LP2-P4	LM1-M3	P2 L	P2 W	P3 L	P3 W	P4 L	P4 W	M1 L	M1 Wm	M1 Wd	M2 L	M2 Wm	M2 Wd	M3 L	M3 Wm	M3 Wd
KLT-638r	–	–	78.6	–	–	17	–	15.9	19.9	22	22.1	24.8	27.1	24.3	23	30.3	21.3	20.6
KLT-638l	–	–	78.3	–	–	16.8	17	15.3	19.4	22.4	22.4	25.2	27.2	23.6	23.8	29.95	20.6	19.3
KLT-869	–	–	87.1	19	11.9	–	–	–	–	29.1	18.4	19.3	31.5	19.7	18.3	31	18	–
KLT-319	–	–	93.65	–	–	–	–	19.3	–	29.3	22.4	24.9	32	21	–	30.5	20	–
TSR-161r	149	58.95	88.9	20	13.8	22.3	15.6	19.7	20.5	27	20.1	20.7	30.1	20.6	19.6	30.8	19.9	18.5
TSR-161l	152	62.3	90.5	19.8	13.9	21.5	16.8	19	19.6	28.2	20.2	20.4	30.9	21.3	20.8	31.2	20.3	19.1
TSR-D17-7	–	–	–	–	–	18	18.5	17.5	23.1	23.8	–	–	30.5	28.2	28.7	–	–	–
TSR-D20-10	–	–	–	–	–	–	–	–	–	–	–	–	32.4	22.8	–	30.6	21.2	19
TSR-E21-45	–	–	–	–	–	–	–	19.2	–	27	24.3	25.6	29.9	25.6	23.8	27.9	24.6	22.7
APL-419	135	56.5	81.55	19.5	14.6	20.3	17.6	17.6	20.5	23	26	26.9	29.5	26.6	27.2	31	26	29.7
APL-269	136	58.9	77	19.2	13	20.5	17.5	19.6	21.3	22	24.6	26.2	26.2	27	26.3	29.3	26	25
APL-746	150	58.7	88.8	16.4	13.2	18.5	16.7	18.5	18.1	28.3	24.5	22.9	29	20.8	19.8	28.9	19.6	–
APL-34	–	–	77.45	–	–	19.1	17.3	17.5	22	22	26.3	27.5	27.5	28.2	28	31	27.5	25.8
APL-433	–	–	–	–	–	–	–	–	–	26.8	26.5	24.6	32.4	23.8	21.6	33	21.5	18.5
APL-432	–	–	80.15	–	–	–	–	16	21.9	23	26.8	27.5	28.5	27.25	26.3	32	26.3	24.3
APL-484	–	–	80.9	–	–	–	–	–	–	22	25.5	28	26.3	28.1	27.7	30.8	26	23.5
APL-270	–	–	81.44	–	–	–	–	–	–	22.5	25.3	25.1	29.3	26.2	23.5	29.8	24.4	21.6
APL-448	–	–	79.3	–	–	–	–	–	–	–	24.8	27.8	25	28.4	29.2	28.7	26.3	27.3
APL-487	–	–	–	–	–	–	–	–	–	–	–	–	29	27.1	26.5	32.7	27.7	24.4
APL-505	–	–	–	–	–	–	–	–	–	29.5	18.7	20.3	33.6	19.5	17.8	–	–	–
APL-264	–	–	–	–	–	19.1	15.3	18	20.7	–	–	–	–	–	–	–	–	–
APL-313	–	–	–	–	–	–	–	–	–	23.5	–	–	25.6	–	–	–	–	–
APL-443	–	–	–	19.4	14	–	–	–	–	–	–	–	–	–	–	–	–	–
APL-441	–	–	–	20.7	12.8	–	–	–	–	–	–	–	–	–	–	–	–	–
APL-152	–	–	–	–	–	23.5	22.2	–	–	–	–	–	–	–	–	–	–	–
APL-442	–	–	–	–	–	18.3	19.3	–	–	–	–	–	–	–	–	–	–	–
APL-512	–	–	–	–	–	19.2	19.2	–	–	–	–	–	–	–	–	–	–	–
APL-513	–	–	–	–	–	22.3	17.2	–	–	–	–	–	–	–	–	–	–	–
APL-511	–	–	–	–	–	18.7	18.5	–	–	–	–	–	–	–	–	–	–	–
APL-510	–	–	–	–	–	–	–	18	20.7	–	–	–	–	–	–	–	–	–
APL-509	–	–	–	–	–	–	–	16.2	20.8	–	–	–	–	–	–	–	–	–
APL-749	–	–	–	–	–	–	–	17.3	21.3	–	–	–	–	–	–	–	–	–
APL-399	–	–	–	–	–	–	–	–	–	33.6	22.4	23.7	–	–	–	–	–	–
APL-497	–	–	–	–	–	–	–	–	–	33.9	20.8	22.3	–	–	–	–	–	–
APL-748	–	–	–	–	–	–	–	–	–	–	–	–	29.6	29.6	29.2	–	–	–
APL-495	–	–	–	–	–	–	–	–	–	–	–	–	35.9	25.3	23.4	–	–	–
APL-472	–	–	–	–	–	–	–	–	–	–	–	–	–	–	–	32.6	28	26.1
APL-240	–	–	–	–	–	–	–	–	–	–	–	–	–	–	–	32.1	25.7	25.2
APL-263	–	–	–	–	–	–	–	–	–	–	–	–	–	–	–	31.1	25.4	22.6
APL-747	–	–	–	–	–	–	–	–	–	–	–	–	–	–	–	31.6	29.1	28.6

Appendix 3B	Lp2-m3	Lp2-p4	Lm1-m3	p2 L	p2 W	p3 L	p3 W	p4 L	p4 W	m1 L	m1 Wm	m1 Wd	m2 L	m2 Wm	m2 Wd	m3 L	m3 Wm	m3 Wd	m3Wp
KLT-177	–	–	84.6	–	–	20.3	–	19.1	10.8	20.4	14.9	16	25.6	–	–	37.1	16.3	16.3	9.3
KLT-318	155	53	102.5	–	–	18.6	12.8	22.6	13.7	25	16.6	17.2	31.8	19.3	–	45.1	17.9	17.2	10.2
TSR F20-16	–	60.8	93.8	15.6	10.3	20.2	11.5	22.5	11.25	27.9	15.5	16.6	28.3	18.1	17.8	37.6	16.4	17.4	9.9
TSR D20-8	–	–	93.9	–	–	–	–	26.1	13.1	–	–	16.1	29	16.7	17.4	41.7	15.3	17.1	7.8
TSR E19-27	–	–	–	–	–	–	–	–	–	–	–	–	–	–	–	39.9	17.8	17.4	9.7
TSR E19-26	–	–	–	–	–	–	–	–	–	–	–	–	29.5	18.7	17.5	–	–	–	–
KRI-36	–	–	–	11.4	–	19.8	11.6	–	–	–	–	–	–	–	–	–	–	–	–
KRI-37	–	–	–	–	–	–	–	21.3	12.6	–	–	–	–	–	–	–	–	–	–
KRI-35	–	–	–	–	–	–	–	–	–	–	–	–	–	–	–	39.1	16.2	16.7	8
APL-478	143	51	88.6	12.7	9.1	18.7	11.6	20.4	14.7	22	15.9	17	27.5	18	18.5	38.8	17.6	18.1	12.6
APL-27	–	–	–	–	–	18.7	11.1	22	13.2	–	–	–	27.2	18	18.6	38.8	17.7	16.1	9
APL-259	–	–	91.8	–	–	–	–	22.7	12.5	25	15.5	15.3	29	16	15.7	39.7	15	15.1	8
APL-477	–	56.2	–	13	8.4	20.9	11.4	23.6	12.5	24	15.6	16.8	–	–	–	–	–	–	–
APL-189	–	–	–	–	–	18	10.7	22	13.4	–	–	–	–	–	–	–	–	–	–
APL-479	–	–	–	–	–	–	–	–	–	–	–	–	27.3	16.5	18	41.8	16.3	15.6	8.3
APL-503milk	–	–	–	–	–	–	–	–	–	30.7	14.4	14.8	–	–	–	–	–	–	–
APL-456milk	–	–	–	–	–	–	–	–	–	32.5	14.4	14.9	35.5	14.9	14.9	–	–	–	–
APL-421milk	–	–	–	–	–	–	–	–	–	32.6	13.5	13	–	–	–	–	–	–	–
APL-422milk	–	–	–	–	–	–	–	–	–	31.8	13.2	13.3	–	–	–	–	–	–	–
APL-493milk	–	–	–	–	–	–	–	–	–	32.3	13.6	13.6	–	–	–	–	–	–	–
APL-753milk	–	–	–	–	–	–	–	–	–	32.4	–	13.4	–	–	–	–	–	–	–

Appendix 3 (continuation). — Dental and metapodial measurements of the Mygdonia early bison. **C,** metacarpal III+IV; **D,** metatarsal III+IV. Abbreviations: **Elem.**, element; **f**, female; **m**, male. **Metapodial measurements**: **MLEN**, maximum length; **PAP**, proximal epiphysis anteroposterior diameter; **PML**, proximal epiphysis mediolateral (transverse) diameter; **MAP**, midshaft (determined using MLEN) anteroposterior diameter; **MML**, midshaft mediolateral diameter; **MVAP**, medial trochear verticilli anteroposterior diameter; **LVAP**, lateral trochlear verticilli anteroposterior diameter; **EMAP**, external margin of medial trochlea anteroposterior diameter; **ILAP**, internal margin of lateral trochlea anteroposterior diameter; **AVML**, anterior aspect of trochlear verticilli mediolateral diameter; **IVML**, distal mediolateral diameter of trochlear verticilli; **PVML**, posterior aspect of trochlear verticilli mediolateral diameter; **IDML**, inferior aspect of distal epiphysis greatest mediolateral diameter; **DDML**, diaphysis distal end (metaphysis) mediolateral diameter. For measurement abbreviations, see also Maniakas & Kostopoulos 2017a: fig. 2. Measuremens **in red** represent best estimations.

APPENDIX 3C	Sex	Elem.	Side	MLEN	PAP	PML	MAP	MML	EMAP	MVAP	LVAP	ILAP	AVML	IVML	PVML	IDML	DDML
Specimen Apollonia 1																	
APL-96	f	MC	left-y	226.25	38.82	66.07	27.24	35.73	29.79	37.77	36.77	34.81	29.31	33.23	34.48	66.48	64.89
APL-230	f	MC	left	–	39.86	62.61	29.85	40.18	–	–	–	–	–	–	–	–	–
APL-258	f	MC	left-y	–	32.92	57.71	23.52	31.82	–	–	–	–	–	–	–	–	–
APL-95	f	MC	left	246.51	42.06	68.75	29.18	38.93	29.87	40.26	40.11	35.62	28.94	32.87	34.26	–	69.19
APL-312	f	MC	left	–	40.43	59.79	–	–	–	–	–	–	–	–	–	–	–
APL-276	f	MC	left-y	–	40.72	64.85	27.88	36.67	–	–	–	–	–	–	–	–	–
APL-677	f	MC	left	244.81	40.47	67.04	28.42	41.25	29.55	38.44	38.47	35.07	25.82	31.73	33.56	68.6	65.83
APL-208	f	MC	left	–	–	–	–	–	29.05	38.82	37.61	35.29	28.03	32.59	33.22	64.58	63.48
APL-79	f	MC	left	–	–	–	–	–	28.15	36.96	36.39	34.18	25.64	31.07	32.09	64.68	62.03
APL-51	f	MC	right	–	38.28	64.04	–	–	–	–	–	–	–	–	–	–	–
APL-257	f	MC	right	–	–	–	–	–	29.46	36.03	36.25	33.82	28.08	36.78	32.48	70.77	66.05
APL-262	f	MC	right	234.76	38.68	65.21	29.59	41.06	30.86	39.88	38.61	36.27	26.66	31.37	32.87	65.08	62.82
APL-196	f	MC	right-y	233.73	34.62	62.86	25.62	36.09	26.72	34.43	–	–	25.42	28.87	29.52	59.53	59.41
APL-373	f	MC	right	235.41	39.62	65.49	29.61	42.96	27.89	36.73	37.03	35.77	27.18	29.92	33.27	66.77	65.65
APL-745	m	Mc	left-y	244.5	–	–	28.71	42.08	29.2	38	41.2	36.5	34.3	36.2	37.4	76.2	70.25
APL-738	m	MC	left	239.94	39.92	70.53	31.11	46.69	–	38.39	39.13	–	29.36	35.08	36.76	–	–
APL-578	m	MC	left	252.56	42.11	69.18	33.52	51.17	30.38	42.07	42.51	38.33	30.28	35.22	35.93	76.04	73.11
APL-520	m	MC	left	–	44.06	76.02	32.06	47.92	–	–	–	–	–	–	–	–	–
APL-414	m	MC	right	244.93	41.58	70.32	34.11	45.39	32.51	41.87	42.09	37.88	29.69	35.22	36.95	76.38	71.14
APL-201	m	MC	right	–	–	–	–	–	34.88	48.18	45.05	44.29	33.61	42.71	–	88.81	83.62
APL-654	m	MC	right	–	–	–	–	–	31.51	42.89	41.23	38.66	29.09	34.21	35.82	66.17	65.98
APL-446	m	MC	right	243.06	43.51	71.15	31.36	49.48	31.84	41.71	40.48	39.77	29.94	34.54	37.09	72.69	70.63
APL-719	m	MC	right	258.11	48.37	78.26	32.18	49.56	33.72	42.83	43.18	40.67	33.36	39.53	40.86	79.96	76.49
TSR D18-42	?m	MC	left	236.5	37.9	69.7	28.6	43	29	36.6	36.5	34.6	32.3	32.8	35.4	70.1	67.7
TSR F18-55d	f	MC	right	225.4	40.8	65.2	25.7	37.8	28.38	37.3	37.11	33.1	29.6	32.7	31.5	64.7	60.7
TSR E17-24	?	MC	left	223.9	42.1	65	26.5	38	28.4	38.5	37.6	34.4	30.15	32.3	33.15	65.4	63.3
KRI-25	f	MC	left	220.65	38	67.65	28	43.3	26.8	–	37.4	32.9	29.9	34	35.7	65.8	63.8
KRM	m	MC	left	253.5	38.5	73.7	35.2	46	30.6	39.7	39.8	37.6	33.4	34.2	36	70.8	70.7
KLT-305	f	MC	right	227.42	39	64.4	27.34	41.5	27.8	37.6	37.9	33.8	29.5	33.8	36.5	69.17	64.2
KLT-646	m	MC	right	239.82	39	72.7	30.6	48.1	–	–	36.4	34.6	35.95	39.9	–	77.46	–

APPEND. 3D	Sex	Elem.	Side	MLEN	FLEN	PAP	PML	MAP	MML	EMAP	MVAP	LVAP	ILAP	AVML	IVML	PVML	IDML	DDML
APL-82	m	MT	left	–	–	63.97	–	–	–	–	–	–	–	–	–	–	–	–
APL-66	m	MT	left	286.86	268.43	55.96	62.13	40.31	38.13	28.48	39.31	38.11	38.23	33.97	36.44	34.58	70.64	68.82
APL-603	m	MT	right	281.68	260.24	61.21	59.35	38.53	36.49	30.44	40.93	40.26	38.83	29.95	34.46	35.52	67.68	66.79
APL-194	m	MT	left	286.21	269.08	59.55	58.31	35.68	33.63	29.69	40.51	39.11	37.11	29.72	33.36	34.14	66.43	64.47
APL-197	m	MT	left young	–	–	–	–	34.24	33.54	–	–	–	–	–	–	–	–	65.29
APL-94	m	MT	left	278.13	261.53	55.74	57.33	39.74	35.89	29.98	39.85	37.71	36.52	33.25	30.91	28.85	60.57	64.71
APL-200	f	MT	right	268.22	251.71	51.38	53.57	–	–	28.92	37.82	37.33	35.57	29.54	32.06	32.11	62.54	62.59
APL-521	f	MT	right	270.07	252.81	52.48	54.98	34.69	34.23	29.47	40.64	39.12	37.33	28.43	31.42	33.29	59.48	61.29
APL-41	f	MT	left	271.37	252.88	53.54	53.86	33.66	31.74	30.02	39.78	38.04	36.91	28.41	32.06	32.96	63.76	60.43
APL-192	f	MT	right	261.25	243.27	52.14	53.13	36.08	31.07	27.71	36.86	35.28	34.09	28.37	31.62	31.74	61.11	57.31
APL-249	f	MT	left	270.93	251.91	53.27	57.03	33.27	38.14	28.96	39.05	?	34.07	29.58	31.81	32.31	63.05	60.98
APL-97	f	MT	right	280.19	258.68	56.09	53.78	33.72	33.21	29.51	38.83	39.11	36.17	27.61	31.57	31.24	64.66	60.74
APL-718	f	MT	left young	–	–	–	–	31.91	32.86	28.41	38.13	36.71	35.48	28.06	31.96	32.11	61.56	63.43
APL-391	f	MT	left	–	–	53.14	53.03	34.25	33.77	–	–	–	–	–	–	–	–	–
APL-101	f	MT	right	–	–	51.89	53.42	–	–	–	–	–	–	–	–	–	–	–
APL-80	f	MT	left	–	–	53.36	53.48	–	–	–	–	–	–	–	–	–	–	–
APL-207	f	MT	left	–	–	54.11	51.07	–	33.17	–	–	–	–	–	–	–	–	–
APL-107	f	MT	right	–	–	52.43	53.06	–	–	–	–	–	–	–	–	–	–	–
APL-294	f	MT	right	–	–	55.43	56.84	33.16	31.72	–	–	–	–	–	–	–	–	–
APL-193	f	MT	right	–	260.06	–	–	34.03	37.41	28.81	38.66	37.15	35.87	28.52	30.64	31.94	62.66	61.23

Appendix 4. — Palaeodemography of the Apollonia bison. An attempt to reveal the basic paleodemographic characteristics of the early bison population from Apollonia is given here. The Apollonia early bison is by far much better sampled than bisons from other sites in Mygdonia Basin, represented by 155 specimens (Number of Identified Specimens, **NISP**) from a total of 760 (20.4%), and the second most abundant herbivore after horses in this particular fossil assemblage. Minimum Number of Individuals (**MNI**) and the corresponding NISP for the metacarpal bones, upper and lower toothrows are given in Appendix 4A.

Appendix 4A. — Minimum Number of Individuals (**MNI**) and Number of Identified Specimens (**NISP**) of the early bison populations from the Mygdonia Basin based on dental and postcranial data. Young individuals of this table are those retaining a milk dentition. For toothrows MNI counts of right (**r**) or left (**l**) specimens per age class (thus, the MNI for two upper right toothrows with same dental combination but of different wear stage is scored as 2). Symbol: *, independently of sex. Abbreviations: **APL**, ; **KLT**, Kalamoto-2; **TSR**, Tsiotra Vryssi.

	Upper toothrows			**Lower toothrows**			**McIII+IV**	
Appendix 4A	**MNI young**	**MNI adult**	**NISP (r+l)**	**MNI young**	**MNI adult**	**NISP (r+l)**	**MNI***	**NISP (r+l)**
APL	10	10	26	6	4	15	15	23
TSR	–	3	5	-	3	3	1	1
KLT	1	2	4	-	2	2	2	2

Based on upper toothrows we estimate the MNI of Apollonia bison at 20 individuals, including calves and adults, with an apparent equilibrium between them. On the contrary from 15 individuals based on metacarpals only 4 represent calves (26.6%) but it is possible that fusion of distal epiphysis of metacarpals achieved earlier in life than permanent dentition.

According to our results, the best metrical variables that discriminate sexually metacarpals are the anteroposterior extend of the proximal epiphysis (PAP) and the middle diaphysis diameters (MAP and MML; see Maniakas & Kostopoulos 2017a: fig.2). Thus specimens with a PAP > 41 mm, MAP > 30 mm and MML ≥ 45 mm (or those meeting simultaneously two of the three conditions) are classified as males. An additional group of distal metacarpals was also classified according to the comparison of their distal metrical dimensions with the corresponding male and female ranges provided by the previous sexual grouping. Thus APL-79, 208 and 257 were classified as females while APL-201 and 654 as males. The specimen APL-745 shows a rather slender diaphysis but already a widened distal epiphysis that approach better males and therefore it is provisionally referred to as a young male individual. Based on these metrical discrimination we assume 14 metacarpals as belonging to females and 9 to males.

Morphological sex discrimination among metatarsals appears more difficult, whereas metrical distinction is sometimes risky due possibly to the fact that some adult female individuals overlap in size with males in late adolescence and with already fused epiphyses. The best metrical variables that discriminate sexually metatarsals are the total length (MLEN), the anteroposterior and mediolateral extend of the proximal epiphysis (PAP, PML), the middle diaphysis deepness (MAP) and the mediolateral extend at the distal epiphysis (DDML; see also Maniakas & Kostopoulos 2017a: fig. 2). Thus, specimens with a MLEN < 280 mm, PAP < 56 mm, PML < 57 mm, MAP < 35 mm, and DDML < 64 mm (or those meeting simultaneously three of the six conditions) are classified as females. Based on this metrical discrimination we suggest 14 metatarsals as belonging to females and 6 to males.

According to the sex determination for metacarpals, the MNI of females is estimated at 9 individuals vs 6 for males (8 and 5 for metatarsals respectively), making the relation males:females approximately 2:3. Although the bison association from Apollonia is unlikely to represent a single momentum from the animal's life, the predominance of females and the high percentage of calves are rather indicative of a mixed maternal herd analogous in size and combination to that observed in extant bisons (McHugh 1958; Reinhardt 1985).

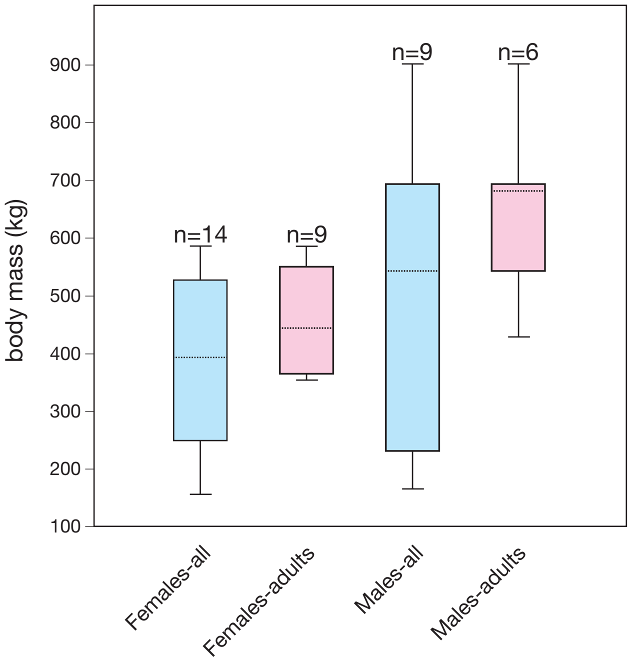

Appendix 4B. — Box plot of the body mass variation per sex of the Apollonia bison population based on metacarpals. Average body mass estimation (ABME) per results from the three individual body mass estimations produced by PML, PAL, and IDML linear variables of metacarpals (see Maniakas & Kostopoulos 2017a: fig. 2).

Body mass predictions based on metacarpals (following Scott 1983) allow us to evaluate the degree of sexual dimorphism on body size in the Apollonia bison. Calves of both sexes are rather small, weighing between 150 and 350 kg. Average body mass is 654.6 kg for males (n=6; or 517.5 kg including calves, n=9) and 466.1 kg for females (n=9; or 379.0 kg including calves, n=14) (Appendix 4B). The obtained values are very similar

Appendix 4C. — Sexual dimorphism index (based on the metacarpal III+IV linear variables: MLEN, PML, MML; e.g. Maniakas & Kostopoulos 2017a: fig. 2) in Apollonia early bison population in comparison with *Bison priscus* Bojanus, 1827 and extant species (method and data according to Drees 2005).

	APL (n=12-17)	***B. bonasus* (n=29)**	***B. bison* (n=15)**	***B. priscus* (n=18)**
MLEN	4.2	3.7	6.1	2.8
PML	11.7	13.9	20.4	13.1
MML	19.3	21.7	27	19.6

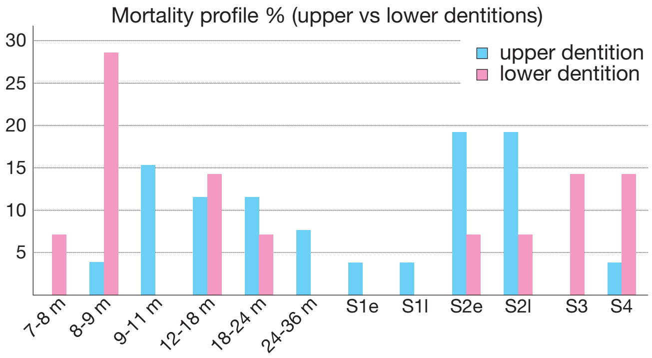

Appendix 4D. — Mortality profiles of the Apollonia bison population based on the percentages of deaths per age class as inferred from upper and lower dentitions. Abbreviations: **m**, age in months; **S**, age classes following Skinner & Kaisen (1946); **e**, early; **l**, late.

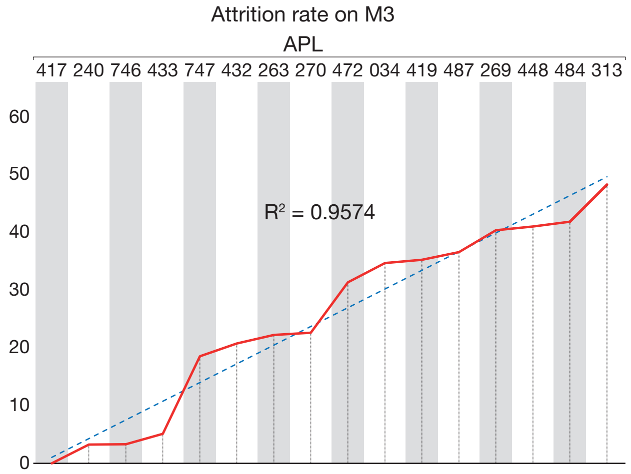

Appendix 4E. — Attrition rate on the M3 of Apollonia early bison population.

to the means and ranges of males and females of the extant European wisent (*B. bonasus*) and American bison (*B. bison*) (Skinner & Kaisen 1946; Krasińska & Krasiński 2002).

Based on available compete forelimb segments (Humerus-Phalanx III) and by analogy to living bison, we assume the Mygdonia taxon was as tall as extant *B. bonasus* with a rough height estimation at the shoulders approximately 1.9 m for the larger bull of the Apollonia site and 1.65 m for the smallest individual from Tsiotra Vryssi. As in extant bison and wisent, males were slightly taller (*c.* 4% either excluding or including young individuals) but much heavier (40%) on average than females.

Amount of difference between the two sexes of the Apollonia bison (based on metacarpal bones following Schertz 1936; *sensu* Drees 2005; Appendix 4C) are in very good agreement with values obtained for extant *B. bonasus* and Late Pleistocene *B. priscus* from the North Sea (Drees 2005). Increased robusticity of male metacarpals in bisons has been linked to their massive head and shoulder region calling for a stouter front leg (Drees 2005). Nevertheless, early bisons like the Apollonia one (see also Moyà-Solà 1987; Sher 1997) with a presumably lighter cranial region (as inferred by several European crania of early bisons, as well as KLT-638) appear as dimorphic as later species (Appendix 4C), suggesting that sexual dimorphism in such gregarious ruminants cannot be simply related to biomechanics, as directly or indirectly implied by some authors (e.g. Schertz 1936; Lewis *et al.* 2005; Drees 2005). On the other hand, studies on the expression of cranial sexual dimorphism in fossil species such as the well-known *B. antiquus* Leidy, 1852, *B. priscus* or *B. schoetensacki* are missing from the literature in contrast to those for metapodials (e.g. Lewis *et al.* 2005, 2006; Drees 2005).

Given the body size compatibility with extant wisent, a similar life expectancy in wild of 16 years and an analogous dental eruption pattern is assumed for the Apollonia early bison. Analysis of the age structure of the Apollonia bison population is carried out in two ways. In the first approach each upper and lower toothrow is attributed to an age class according to its wear stage (Appendix 4D).

The results from both the upper and lower dentitions indicate high infant mortality affecting individuals younger than 3 years old, especially newly born calves (<1 year), and relatively high mortality late in life, altogether suggesting an attritional mortality model (Klein 1982; Stiner 1990; Steele 2003). The most abundant upper dentitions, exhibit, however, a more complex mortality pattern, revealing relatively more deaths during early maturity (S2 stage) than later (Appendix 4D). As there is no obvious taphonomical reason to explain this condition, we suspect that other factors than natural mortality may contribute to the death of animals at the peak of their sexual and physical maturity.

To further explore the mortality profile, and to normalize for the effect of duration differences in age classes, a second approach is performed where a particular age in months has been attributed to each upper permanent toothrow bearing M3.

The age of an individual (IA) is resulting from the equation:

$$IA = 36 + (Hmax-Hi)*w$$

Where Hmax is the maximum observed height on unworn M3, here represented by the specimen APL-417, the tallest preserved M3 in the Apollonia sample.

Hi is the preserved height of M3 of the specimen/individual in question, and "w" a constant representing tooth wear per month.

To evaluate the constant "w" we assume that the just erupted and unworn M3 APL-417 represents an individual of approximately 36 months old, i.e., the timing the M3 rises on the

Appendix 4F. — Individual age estimation from upper M3 of early Bison from Apollonia, Mygdonia Basin, Greece. Abbreviation: **Hpa**, height of the M3 at the paracone (in mm).

Specimen	Hpa	$H_{(APL417)}$-Hi	Individual Age (in months)
APL-417	55.82	0	36.00
APL-240	52.57	3.25	46.35
APL-746	52.5	3.32	46.57
APL-433	50.7	5.12	52.31
APL-747	37.3	18.52	94.98
APL-432	35.06	20.76	102.11
APL-263	33.6	22.22	106.76
APL-270	33.2	22.62	108.04
APL-472	24.5	31.32	135.75
APL-34	21.16	34.66	146.38
APL-419	20.6	35.22	148.17
APL-487	19.26	36.56	152.43
APL-269	15.5	40.32	164.41
APL-448	14.83	40.99	166.54
APL-484	14	41.82	169.18
APL-313	7.6	48.22	189.57

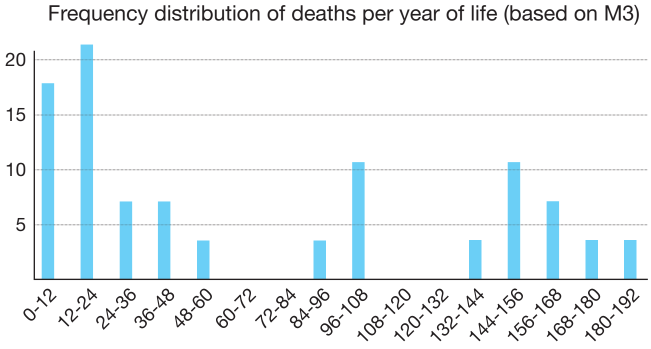

Appendix 4G. — Frequency distribution of deaths per year of life for the bison population from Apollonia as inferred from the wear stage of M3s.

similarly weighted extant taxa (Skinner & Kaisen 1946; Wegrzyn & Serwatka1984), while the specimen APL-313 with fully worn molars represents an individual at the very end of its life, that is 16 years or 192 months by analogy to extant bison and wisent living in the wild. Thus:

$$\begin{aligned} w &= \text{HM3APL-417} - \text{HM3APL-313} / (192-36) \\ &= 49/156 \\ &= 0.314 \text{ mm/month.} \end{aligned}$$

Although tooth wear may not be uniform throughout the life of the animal depending on seasonal and other factors, we assume the average annual wear to be rather constant (Appendix 4E). The results of aging Apollonia bison individuals represented by permanent upper toothrows bearing the M3 are given in Appendix 4F.

As previously, the frequency distribution of deaths per year of life (Appendix 4G) shows the highest mortality rates for animals between 0 and 2 years old followed by animals of 8-9 years and 12-13 years old. In a three-age system (e.g. Stiner 1990; Discamps & Costamagno 2015) juveniles represent 53.6%, prime adults 17.8% and old adults 28.6% in the Apollonia bison thanatocoenosis. These proportions classify the mortality profile of APL bison in the Juveniles-Old-Prime (JOP) zone of Discamps & Costamagno (2015) suggesting a U-shaped profile that may result from a variety of causes (disease, malnutrition, accidents) but most likely by a predation strategy comparable to that of living social cursorial carnivores such as wild dogs and spotted hyenas; both group

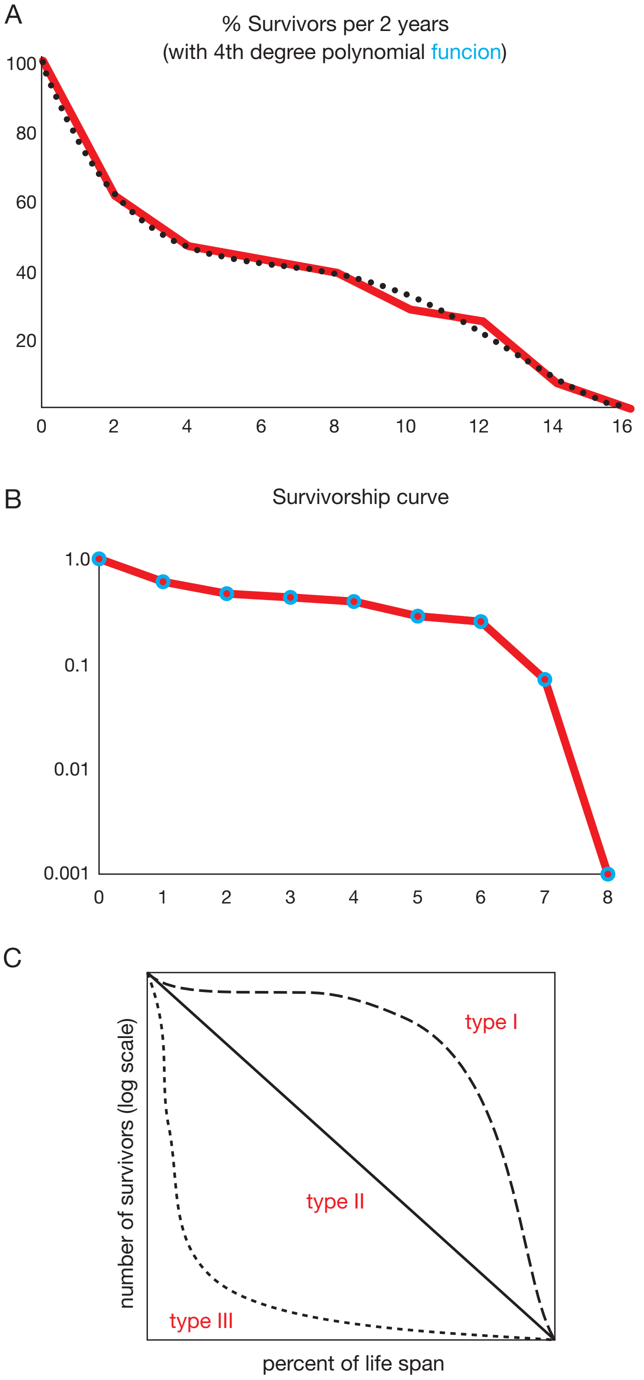

Appendix 4H. — Survivors per 2-years (**a**) and corresponding survivorship curve (**b**) of the Apollonia bison population, against standard types of survivorship curves (**c**). The survivors per 2-years curve (red solid line in **a**) best fits a fourth degree polynomial function model (dotted line in **a**). The survivorship curve of the Apollonia bison population (**b**) does not match any of the three standard types (**c**; see text).

of predators appear to have a strong signal in the fauna of Apollonia where pachycrocutid hyaenas and at least two wolf-like canids are present (Koufos & Kostopoulos 1997; Koufos 2018). The high percentage of spiral fractures on long bones and some carnivore marks strengthen this possibility.

The "survivors per year" (Appendix 4H[a]) and survivorship curves (Appendix 4H[b]) show a sigmoidal pattern: high neonate mortality is followed by a period of relative stability until the last quarter of lifespan when relative survivorship drops abruptly down. This pattern does not match any of the three classical models of survivorships (Type I, II, III; Fig. 11C) but it is fully compatible with that provided for other terrestrial mammals (Kurtén 1953; Caughley 1965; Erickson *et al.* 2010).